

Correlation between Tsunami Height and Strong Ground Motions

*Anatoly Petukhin¹, Alexander Gusev², Victor Chebrov³

1.Geo-Research Institute, 2.Institute of Volcanology and Seismology, Far East Branch, Russian Academy of Sciences, 3.Kamchatka Branch, Geophysical Service, Russian Academy of Sciences,

When a large earthquake occurs off a coast, the resulting ground motion can soon be followed by the arrival of tsunami waves. This interrelationship can be useful for issuing tsunami alerts. This study aims at detecting correlative relationships between the intensity (runup) of a tsunami at a site along the coast and ground motion parameters at the same site due to the earthquake that produced the tsunami. Our estimates were derived by combining historical and instrumental data for eight sites along the Pacific coast of Japan (Figure 1).

Our regression analysis of collected and systematized data used the tobit model, which is able to incorporate all tsunami data, including censored data below the tsunami-detection threshold. We show that if such tsunamis are neglected by the standard regression model, the result is to overestimate the height of predicted tsunamis (Figure 2).

Analysis of the regression results (Figure 2) shows that when a tsunami generating-earthquake has occurred, a tsunami with runup that is equal to or greater than 50 cm should be expected if peak ground motion velocities greater than 7 cm/s have been recorded at the same site, with the probability of the failure to predict being 16%.

However we should notice that large standard deviation of data, around +/- 4 times, results in large percent of false alarm cases and makes practical prediction problematic. In order to analyze possible reasons of such a large scattering of data, we grouped them according to type of ground condition, shore line and earthquake source. It is found that effects of ground conditions and shore line are minor in comparison with tsunami-genic effect of particular source.

Acknowledgments. Data from databases of next institutions and agencies are used: IVMiMG, NOAA, NIED, JMA, PARI, Tohoku Univ. We are grateful to T.V. Shkinder for help with Japanese text sources. Figure 1. A map of the study area. The triangles mark the selected sites with copious data, with a number of observations of 20 or more. The inclined crosses mark the epicenters of earthquakes analysed.

Figure 2. A summary of tobit regression for individual sites (light lines) and for all of the data at the eight sites combined (long-dashed line). The short-dashed line shows the mean plus standard error for all of the sites combined. The heavy solid line is the mean for the standard regression without the censored data.

Keywords: strong ground motions, tobit regression, tsunami forecast

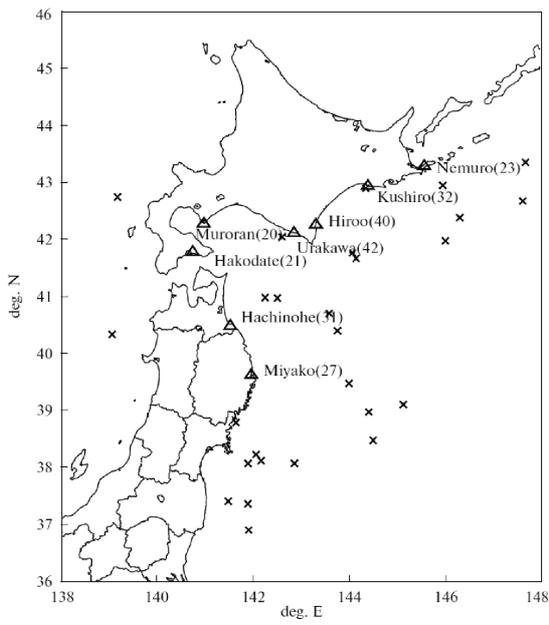


Figure 1

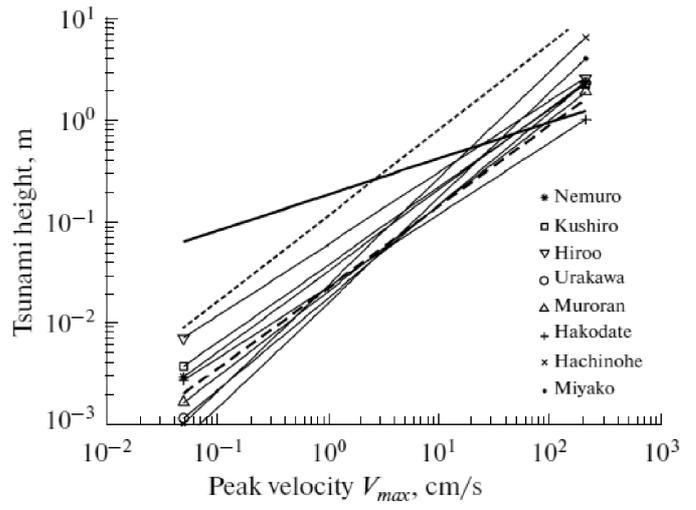


Figure 2

Updated empirical relationship of large tsunami height between offshore and coastal stations

*Yutaka Hayashi¹

1. Meteorological Research Institute

Since the first report (Takayama et al., 1994) on detection of offshore tsunami due to the 1993 Southwest off Hokkaido earthquake, offshore tsunami data detected by Nationwide Ocean Wave information network for Ports and Harbours (NOWPHAS) has been accumulated. My previous study (Hayashi, 2010) derived empirical relationships of tsunami height between offshore and coastal stations from pairs of initial tsunami height or maximum tsunami amplitude data obtained by coastal tide stations and offshore sites of NOWPHAS wave stations or RTK-GPS buoys during eight tsunami events between 1993 and 2007; and then, the ratio of initial tsunami height or maximum amplitude observed at a coastal tidal station on that at the offshore site was found to be proportional to the fourth root of the ratio of the sea-bottom depths from the mean sea level at the offshore sites to the coastal station. However, dataset used by this study has only two pairs from observation data from RTK-GPS buoys each for initial large tsunami and maximum amplitude; and the range of tsunami height in the dataset was limited to between 0.05m and 2.4m. In this study, empirical relationships of tsunami height between offshore and coastal stations are reconstructed by including maximum tsunami height data obtained during 2010 Maule earthquake tsunami (Kawai et al., 2010) and 2011 off the Pacific coast of Tohoku Earthquake tsunami (Kawai et al., 2011). In the 2011 event, some tidal stations were damaged; for these stations measured tsunami inundation heights by field surveys near tidal stations (Abe and Hiramatsu, 2012) are utilized instead, because differences between normal maximum tsunami heights observed at tidal stations and measured tsunami inundation heights by field survey sites near the station are small and within 1m (Hayashi, 2014). The new dataset on pairs of maximum tsunami heights at offshore (GPS buoys or wave) stations and the nearby tidal stations (or field survey site in case of lack of data at tidal stations) shows that the previous equations (Hayashi, 2010), based on the concept that amplification factor is proportional to the fourth root of the ratio of water-depths between at offshore and at onshore stations, severely overestimate amplification factor from offshore to the coast for larger tsunami than 3m at the coast. However, if the saturation of amplification in case of the larger ratio of tsunami height to water depth than 1/3 is assumed, this overestimation can be get rid of. Newly derived empirical relation would improve tsunami height estimation by converting from offshore tsunami height observation or calculation to the nearby coastal points, which are general parts necessary for several ways of tsunami forecasting methodology such as scenario tsunami database (Kamigaichi, 2009) or near-field tsunami forecasting by tFISH algorithm (Tsushima et al., 2009).

Keywords: GPS buoy, Nationwide Ocean Wave information network for Ports and Harbours (NOWPHAS), tidal stations, tsunami amplification factor

Systematic evaluation of performance of real-time tsunami forecasting method based on tsunami source inversion and development of indication for real-time assessment of the tsunami forecasting accuracy

*Hiroaki Tsushima¹, Takeyasu Yamamoto¹

1.Meteorological Research Institute, Japan Meteorological Agency

After the 2011 Tohoku earthquake occurred, offshore tsunami observation networks are expanded around Japan and many researchers are developing tsunami forecasting methods in which the offshore tsunami data are used. We developed a tsunami-forecasting method based on inversion of offshore tsunami waveform data for initial sea-surface height distribution, named tFISH. Forecasting accuracy of tFISH algorithm depends on a spatial relationship between a tsunami source and offshore tsunami stations. This tendency will be strong in tsunami forecasting in the Nankai-trough region and the Japan-trench region before large-scale dense S-net is developed, because the density of offshore tsunami network is biased. This will result in large variety of the timing when the forecasting becomes accurate enough to be used for appropriate update of tsunami early warning. In this presentation, we will show the results of numerical simulations of tsunami forecasting, focusing on the following two points that are important for its practical operation in tsunami early warning system: (1) systematic evaluation of tFISH performance by varying a tsunami source location systematically, (2) development of indication which can assist decision makers of tsunami warning to judge the timing when tFISH-forecasting results become accurate enough to be used for update of tsunami warning.

Keywords: Tsunami early warning, Real-time tsunami forecasting, Offshore tsunami observation, Near-field tsunami, Disaster mitigation, Inverse problem

A trial separation between tsunami height and coseismic deformation from ocean-bottom pressure gauge records using data assimilation method

*Takuto Maeda¹

1. Earthquake Research Institute, the University of Tokyo

Data assimilation method provides a successive estimation of tsunami wavefield rather than the seismic source fault slip or initial sea height. This method avoids ambiguities on inverting source slip, and well assimilates the tsunami also for far-field or tsunami earthquakes without relying on seismic waves, which is preferable and suitable for real-time monitoring and forecasting. The widely-adopted ocean bottom pressure gauge records, however, contain an offset due to coseismic deformation beneath the sensor. This is a common problem among various tsunami real-time forecasting methods, and it made difficult to estimate and/or forecast tsunami until tsunami propagates outside of the source area. This study focuses to separate the coseismic deformation effect from the true tsunami height based on the data assimilation.

First we consider the effect on using tsunami height measured by ocean bottom pressure gauges (hereinafter referred to as pressure height) in linear long-wave tsunami problem. Ocean bottom pressure gauges measure the differential height between the true tsunami height and coseismic deformation, while the true tsunami height obeys the long-wave tsunami equation. The pressure height therefore satisfies the wave equation having inhomogeneous term due to the coseismic deformation. This inhomogeneous term is the origin of offset appeared on the data assimilation with pressure gauge data. The inhomogeneous term contains second-order temporal and spatial derivatives. The former should disappear after the source rupture and arrival of seismic wave, while the latter remains at long elapsed time.

Based on the above understandings of the effect of coseismic deformation, we propose a two-step method to estimate tsunami wavefield based on the data assimilation. First, the pressure gauge data are directly assimilated to the linear long-wave equation. The tsunami height at one-time step future is forecasted by numerical simulation, and the tsunami height at pressure gauge station location is compared with the observed data. The residual between forecast and observation is used to assimilate the surrounding tsunami wavefield by the optimum interpolation method.

Since the data assimilation uses the pressure height, the assimilated tsunami wavefield should be contaminated by the coseismic deformation. As a second step, this contamination effect is eliminated. By numerically calculating the second-order derivatives in space and time from the assimilated tsunami wavefield, we obtain the inhomogeneous term of the wave equation. If we omit the temporal derivative of the coseismic deformation, this inhomogeneous term should obey the Laplace equation of the coseismic deformation, which can be solved numerically. Then the real tsunami height is estimated by subtracting the coseismic deformation term from the pressure height. Though the estimated tsunami flow velocity also was affected by the offset problem, the true tsunami velocity can also be extracted from the derivative of the true tsunami height with respect to space.

A simple 1D numerical experiment for the proposed method was performed. The synthetic tsunami was simulated under the homogeneous sea depth of 3000 m, and recorded at evenly-spaced ocean bottom synthetic stations at intervals of 30 km. At the first step, the data-assimilated tsunami height from pressure height did not detect the initial tsunami due to nearly identical motions between sea bottom and surface. At longer elapsed time the assimilated tsunami height has fictitious negative offset. By applying the second-step of the proposed method, it correctly separated the coseismic deformation, although the result was a little bit wobbled. It is noteworthy that the initial

tsunami rise-up at very early time due to the coseismic deformation was clearly detected by this separation, which could be useful for further shortening the necessary time for forecasting tsunami.

Keywords: Tsunami, Realtime forecasting, Data assimilation, Ocean bottom pressure gauge, Coseismic deformation

Data assimilation of high-density offshore pressure gauge observations for tsunami forecast simulation of the 2012 Haida Gwaii earthquake

*Aditya Gusman¹, Anne F. Sheehan², Kenji Satake¹, Mohammad Heidarzadeh¹, Iyan E. Mulia³, Takuto Maeda¹

1.Earthquake Research Institute, The University of Tokyo, 2.Department of Geological Sciences, University of Colorado Boulder, 3.Department of Ocean Civil Engineering, Kagoshima University, Japan

Here, we use a total of 57 tsunami waveforms recorded on the DARTs and a dense array off Oregon and California from the 2012 Haida Gwaii, Canada, earthquake (Sheehan et al., 2015, SRL) to simulate the performance of two different real-time tsunami-forecasting approaches. In the first approach, the fault slip distribution of the earthquake is estimated by inversion of recorded tsunami waveforms. In the second approach, the recorded waveforms on the dense tsunami array are continuously assimilated to produce tsunami wave fields within the vicinity of the stations. These tsunami source model and tsunami wave fields are then used to estimate the tsunami along the coast of Oregon and California. The dense array provides critical data for both methods to produce timely (> 30 minutes lead time) and accurate (> 94% confidence) in both timing and amplitude of tsunami forecasts.

In the first approach, we use tsunami waveform inversion (Satake et al., 2013, BSSA; Gusman et al., 2015, GRL) to estimate the slip distribution of the 2012 earthquake. The fault geometry is based on the W phase solution for the earthquake. Large slip amounts (4 -5 m) are located near the Haida Gwaii trench. The synthetic tsunami waveforms of the fault slip distribution match well the tsunami observations. Therefore, the fault model is suitable for tsunami warning purposes.

In the second approach, the tsunami waveforms are used in tsunami data assimilation method (Maeda et al., 2015, GRL), which does not require any assumption about the tsunami source mechanism. Tsunami wave field is created at every 1 sec, and it can be used as an input for tsunami forward modeling. Realistic tsunami wave fields begin to emerge after the tsunami passes through 5 stations. As more tsunami data are assimilated, the wave fields from this method are gradually become similar to that produced in the first approach that utilized tsunami waveform inversion.

High accuracies of more than 94% in average are produced from data-assimilation wave field at stations near the shoreline. As an example, using the 130 min data-assimilated wave field, the tsunami waveforms at station FS12B is forecasted with an accuracy of 98% about 30 min in advance. The tsunami data assimilation method that we present can be run continuously in real-time and does not require a fault model. Remarkably, the tsunami forecast accuracy from the tsunami data assimilation method is as good as that from the traditional tsunami forecasting method that assumes a fault model. Real-time tsunami data on dense arrays and data assimilation delivers a new generation tsunami warning system.

Keywords: Tsunami data assimilation, Dense tsunami array, The 2012 Haida Gwaii earthquake tsunami, Tsunami forecast, Earthquake source model

Maximum tsunami height prediction using pressure gauge data by a Gaussian process at Owase in the Kii Peninsula, Japan

*Yasuhiko Igarashi¹, Shin Murata¹, Toshitaka Baba², Ken-ichiro SATO³, Takane Hori³, Masato Okada¹

1.Graduate School of Frontier Sciences, The University of Tokyo, 2.Institute of Technology and Science, The University of Tokushima,, 3.Research and Development Center for Earthquake and Tsunami, Japan Agency for Marine-Earth Science and Technology

In Japan, the Dense Oceanfloor Network System for Earthquakes and Tsunamis (DONET) was recently developed in the Nankai trough (Kaneda et al., 2015). DONET1 is equipped with seismometers and ocean-bottom pressure gauges at 20 points on the sea floor and submarine data can be acquired in real time. We studied the relationship between offshore and coastal tsunami heights with the aim of using DONET1 ocean-bottom pressure gauges for early tsunami prediction.

Previous works focused on the average of maximum absolute values of the hydrostatic pressure changes during a tsunami (Baba et al., 2013). Although compressing time series of pressure gauges data, they revealed a clear relationship between the average waveforms of DONET and tsunami heights at the coast. However, since they assumed linear relationship and used only the average of the data at all the DONET stations, it may be inadequate to take accurate tsunami prediction.

Here, using a standard nonlinear regression method, Gaussian process (GP), we construct an algorithm to predict maximum tsunami height. We found a greatly improved generalization error of the maximum tsunami height by our prediction model. The error is about one third of that by a previous method. Moreover, by optimizing each sensor's weight of GP, we investigate the contributions of each ocean-bottom pressures on the predictions, which enables us to take more accurate prediction of tsunami height and could provide the design criteria of ocean-bottom sensors in the future.

Keywords: Tsunami height prediction, Gaussian Process, DONET

Tsunami height prediction using multiple linear regression and L1 regularization

*Shin Murata¹, Yasuhiko Igarashi¹, Toshitaka Baba², Ken-ichiro SATO³, Takane Hori³, Masato Okada¹

1.Graduate School of Frontier Sciences, The University of Tokyo, 2.Institute of Technology and Science, The University of Tokushima, 3.R&D Center for Earthquake and Tsunami, Japan Agency for Marine-Earth Science and Technology

The Dense Oceanfloor Network system for Earthquakes and Tsunamis (DONET) is constructed in the Nankai trough for real-time earthquakes and tsunamis monitoring (Kaneda et al., 2015). DONET1 has 20 monitoring points with seismometers and ocean-bottom pressure gauges on the ocean floor. It is important to make an accurate estimate of maximum tsunami height from monitoring data of the DONET1, because real-time tsunami forecasting could reduce the damage of tsunami disaster. In previous studies, Baba et al., used linear regression to model the relationship between the maximum tsunami height and the average of maximum absolute values of the hydrostatic pressure (Baba et al., 2013). Although the clear linear relationship has been shown in the previous work, we consider that the prediction is more accurate by using the data observed at all the 20 points rather than using only the average value of the sensors.

We use the data observed at all the 20 stations to make an accurate tsunami prediction by applying multiple linear regression. Multiple linear regression provides the relationship between two or more explanatory variables, e.g. the observed data, and a response variable, e.g. the maximum tsunami height. Moreover, we also adopt L1 regularization. L1 regularization is widely used to identify unnecessary input variables in regression and enables us to find useful sensory points for the tsunami prediction.

We found that the generalization error of the predictions in this study is smaller than that of the previous study. Furthermore, linear regression with L1 regularization provides more accurate predictions. Using L1 regularization, we also found that almost all the sensor constructing DONET1 are necessary for making the prediction and it indicates evidence to the value of all the 20 points DONET stations for tsunami prediction. Furthermore, we compare the linear regression with the nonlinear regression, Gaussian Process (GP) [Igarashi et al., submitted] for the tsunami prediction of expected tsunami scenarios. We found that the linear regression provides better prediction when the prediction data is beyond the observed data.

Keywords: Tsunami height prediction, Linear regression, L1 regularization, DONET

GNSS-based height positioning derived from multiple ships for measuring and forecasting great tsunamis

*Daisuke Inazu¹, Takuji Waseda², Toshiyuki Hibiya³, Yusaku Ohta⁴

1.UTokyo Ocean Alliance, The University of Tokyo, 2.Graduate School of Frontier Sciences, University of Tokyo, 3.Graduate School of Science, University of Tokyo, 4.Research Center for Prediction of Earthquakes and Volcanic Eruptions, Graduate School of Science, Tohoku University

We investigate GNSS-based ship height positioning for measuring and forecasting great tsunamis. We first examined a GNSS height positioning record of a running research vessel. If we use the Precise Point Positioning (PPP), tsunamis greater than 10^1 cm will be detected by ship height positioning. We refer an Automatic Identification System (AIS) data, and find that tens of tankers and cargos are usually navigating over the Nankai Trough. We assume that a future Nankai Trough great earthquake tsunami is measured by PPP-based height positioning of the AIS-derived ship distribution, and examine the tsunami forecast skill of the tsunami measurement by the PPP-based ship height. A method of Tsushima et al. (2009, 2012) is used for the forecast. The tsunami forecast tests were carried out using simulated tsunami data by the PPP-based ship height of 92 tankers/cargos, and by existing ocean-bottom-pressure and GPS-buoy observations over the Nankai Trough at 71 stations. The forecast skill using the PPP-based height of the 92 ships is shown to be comparable to that using the existing offshore observatories at the 71 stations. During the great earthquakes, we suppose that stations along a certain coast that receive successive ship information (AIS data) would fail and obtain no ship data due to the strong ground motion, especially near the epicenter. Such a situation will significantly worsen the skill of the tsunami forecast above. On the other hand, real-time analysis of seismic/geodetic data would be carried out for estimating a tsunamigenic fault model, independently from analyzing offshore tsunami data. Incorporating the seismic/geodetic fault model estimation into the tsunami forecast above possibly compensates the deteriorated forecast skill.

Keywords: GNSS, ship height, tsunami forecast

Development of ensemble tsunami inundation forecasting method using ABIC

*Tomohiro Takagawa¹, Takashi Tomita¹

1. Port and Airport Research Institute

An ensemble forecasting method for tsunami inundation is proposed. The method consists of three elemental techniques. The first is a hierarchical Bayesian inversion using Akaike's Bayesian Information Criterion (ABIC). The second is Montecarlo sampling from probability density function. The third is ensemble analysis of tsunami inundation simulations on multiple tsunami sources with the consideration of source uncertainty. Simulation based validation of the method was conducted. On a case of tsunami generated by a great Nankai trough earthquake, tsunami inundation around Nagoya Port was estimated by using tsunami waveform data of offshore GPS buoys. The error of estimation of tsunami inundation area was about 10% even if we used only ten minutes observation data. The estimation accuracy of waveforms on/off land and spatial distribution of maximum tsunami inundation depth is demonstrated.

Keywords: ensemble forecast, ABIC, Tsunami

Characterized Fault Models for Probabilistic Tsunami Hazard Assessment in the Sagami Trough

*Tadashi Kito¹, Kenji Hirata², Hiroyuki Fujiwara², Nobuyuki Morikawa², Masaki Osada², Makoto Nemoto¹, Hisanori Matuyama¹, YASUHIRO MURATA³, Shinichi Akiyama⁴

1.OYO Corporation, 2.NIED, 3.KOKUSAI KOGYO CO., LTD, 4.CTC

NIED (National Research Institute for Earth Science and Disaster Prevention) has been conducting the project on the probabilistic tsunami hazard along the coastline in Japan (Fujiwara et al., 2013, JpGU). We have already constructed characterized fault models and made tsunami hazard curve using tsunami heights along the coastline estimated by tsunami simulation in the Japan Trench and Nankai Trough. In this study, we have constructed characterized fault models for probabilistic tsunami hazard assessment in the Metropolitan area.

The Philippine Sea Plate and the Pacific Plate subduct beneath the Metropolitan area. The long-term evaluation by the Headquarters for Earthquake Research Promotion (2014) categorizes the earthquakes along the plate boundary between the North America Plate and the Philippine Sea Plate as "M8-class earthquakes along the Sagami Trough". We have modeled these earthquakes as specified fault models. The 1703 Genroku and the 1923 Taisho Kanto earthquakes are involved in this category and M8.6 earthquake with the rupture area of the whole region determined by the Headquarters for Earthquake Research Promotion is the maximum size in this study. The long-term evaluation divided the estimated source area into 5 sub-regions, and we combined these sub-regions adding 2 extra regions that correspond to the source areas of "the 1703 Genroku earthquake" and "the 1703 Genroku - the 1923 Taisho earthquake". We constructed 126 specified fault models in the 11 regions in total. Heterogeneities in the slip amount are expressed using 3 kinds of slip area, called background slip area, large slip area and super large slip area. The large slip area has 2 times of average slip amount and 30% of total fault area, and the super large slip area has 4 times of average slip amount and 10% of total fault area. If the fault area reaches the trench, super large slip areas may be incorporated. The aspect ratio of large slip areas and super large slip area is one to two, and overlap ratio between neighboring large slip areas is approximately 50%.

Because it is quite difficult to specify the source area of M7-class earthquakes caused by the subducted plate along the Sagami trough (long-term evaluation, 2014), we have modeled these earthquakes as unspecified fault models (928 models) with large slip area in the center of the fault that are uniformly distributed in the estimated source area.

We are currently conducting tsunami simulation using the characterized fault models in the Sagami Trough for the tsunami hazard assessment. This study is conducted as a part of the research project "Research on the hazard risk assessment for natural disaster" in NIED.

Keywords: Tsunami Hazard Assessment, Characterized fault model, Sagami Trough

Construction of Fault Model for the Japan Sea Area based on the "Off Shore Fault evaluation Project"

Tsuneo Ohsumi¹, *Kimie Norimatsu², Hisanori Matsuyama², Hiroyuki Fujiwara¹

1.NIED, 2.OYO Corporation

The Ministry of Education, Culture, Sports, Science and Technology, Japan was started "Off Shore Fault Evaluation Project" in 2013. In this project, collect the offshore fault survey data, analyse the data by a uniform method and construct data base.

This study is conducted by a subtheme of the Offshore Fault Evaluation Project.

The purposes of this study are construct the fault model based on the geological fault information that analysed by the Japan Agency for Marine-Earth Science and Technology (JAMSTEC). The two types of fault model we constructed that, the "Primary model" and "Consolidated model". The primary model is the fault model based on the fault information from the Offshore Fault project. The consolidated model is considered the possibility of continuing on the fault distribution and consolidate on the deeper part of the fault. The consolidate model is represented the combination of some primary models.

To construct the primary model, we define the following policies for each parameter settings that considered the epistemic uncertainty and aleatory uncertainty.

The "position, length and strikes of the fault" are based on the geological fault information of the Offshore Fault Project and "depths of the top of fault" are at sea bottom. Construct two types of settings for "fault dips". One is use the basic value and thrust fault as 45 degrees, normal fault as 60 degrees, and strike slip fault as 90 degrees. Another setting is use the "apparent dips" from Offshore Fault Project that, shallow part of the fault is steeply dipping that set by the apparent dips from geological data and deeper part is gradual dipping that adjust to be 45 degrees or 60 degrees, on the average of whole fault dips. The "bottom depths of the fault" are two patterns and one is using a 3D velocity structure models presented by this project and another is from previous study of the Japan Sea area. "Fault widths" are set from the relationship between bottom depth of the fault and dip angle, and "fault rakes" were set to thrust fault as 90 degrees., Normal fault as 270 degrees., Right lateral fault as 0 degrees., Left lateral fault as 180 degrees. The "average of fault slips" is set by the empirical relationship between fault area and Mw by Irikura and Miyake, 2001 and we also considered the large slip areas that, 30 % of fault area and twofold average of slip.

The number of primary models, we set was about 240 models and consolidated models that represented the combination of some primary models are about 550 models. For the consolidated models, it was considered the reproductively for previous occurred earthquakes using the tsunami simulations (Ohsumi et. al., 2015: SSJ meeting).

The Offshore Fault Project will be planning for the Nansei Islands area.

Keywords: Off Shore Fault Evaluation Project, fault model, Japan Sea area

Underestimated fault models for 'maximum-class' tsunami in the Japan Sea, resulted from Irikura and Miyake (2001) scaling relation

*Kunihiko Shimazaki¹

1.University of Tokyo

Application of Irikura and Miyake (2001) scaling relation for estimation of seismic moment of a large shallow crustal earthquake occurring on a vertical fault causes underestimation of seismic moment. Seismic deformations of the 1927 Tango, the 1930 North Izu, and the 1943 Tottori earthquakes are evaluated on the basis of Irikura and Miyake (2001) scaling relation and previously estimated fault areas (Abe, 1978; Kanamori, 1973). The scaling formula gives deformations smaller than one-fourth that observed geodetically.

Keywords: 'maximum-class' tsunami, Japan Sea, scaling relation

Suspension of marine sediment and materials caused by tsunami in Osaka Bay

*Mitsuru Hayashi¹, Satoshi Nakada²

1.Research Center for Inland Seas, Kobe University, 2.Graduate School of Maritime Sciences, Kobe University

The Nankai Trough Earthquake will hit within 30 years, and a huge tsunami will be caused. Marine sediment will be suspended and transported by the tsunami. Not only cysts but also heavy metals are contained in the marine sediment in the inner part of Osaka Bay. We calculated the temporal variation of concentrations of heavy metals, nutrients and so on in the water column while a tsunami caused by the Nankai Trough Earthquake attacks Osaka Bay, and discussed these characteristics. When huge tsunami attacks Osaka Bay, marine sediment will be suspended and there is possibility that the concentrations of heavy metals exceed the environmental criteria for the seawater.

Keywords: Tsunami, Marine sediment , Suspension

Analysis of eddy fields for the vessel evacuation from the giant tsunami

*Satoshi Nakada¹, Mitsuru Hayashi², Ei-ichi Kobayashi¹, Shunichi Koshimura³

1.Graduate School of Maritime Sciences, Kobe University, 2.Research Center for Inland Seas, Kobe University, 3.International Research Institute of Disaster Science, Tohoku University

The Japanese government reported that Nankai Trough Earthquake will occur about 70 % of probability within 30 years in the future and drive the giant tsunami. The speed of the tsunami plus the tidal currents may exceed 2 knot (approximately 1 m/s) at many ports in the Japanese coasts facing to Pacific. Not only this speed but also eddies generated around the nearshore seas can make difficult to operate the marine vehicles and escape from the port that the tsunami attacks according to the evacuation scenarios for ships. The number of commercial vessels present in Osaka Bay was counted using the entry record of vessels and is approximately 100 vessels throughout the year. The ports of Sakai-Senboku, Osaka and Kobe located in the bay head are rank as international hub ports. Various vessels, oil tankers, LNG (liquefied natural gas) carriers, bulk carriers, and PCC (pure car carriers) enter the port of Sakai-Senboku to transport to petrochemical complexes. The influence of eddies should be considered when planning the vessel evacuation manual. This study clarified the characteristics of eddies in Osaka Bay generated by the giant tsunami caused by the Nankai Trough Earthquake, and the influence on vessel evacuation was discussed, especially for the port of Sakai-Senboku, which plays the role of an important lifeline.

We conducted the tsunami simulation with a horizontal resolution of 50 m by employing the nesting method to represent the complex coastal lines around the landfills along the bay coast in Osaka Bay. We used the shallow water equation model with the time step 0.5 seconds to predict the tsunami speed and height during the period from the earthquake occurrence to 600 minutes.

The simulated results showed that the spatial characteristics of eddies generated by the tsunamigenic earthquake around the Port of Sakai Senboku ranged in 900-2500 m during 600 minutes after the earthquake, indicating several times the length of a vessel. The location of eddies are largely fixed. The location of vessels recorded by AIS (Automatic Identification System) from September 1st to 8th, 2012 indicated the major fairways that most vessels enter at the hub ports. The strong eddies were generated in these fairways in the hub port. In particular, the eddies with the more than 2 knot were found in the entrance of the hub port. The vorticity generated in the entrance of the port of Sakai-Senboku can prevent stable navigation. The area-averaged vorticity around the ports increased from 80 minutes after the earthquake and gradually decreased from the approach of the second wave of tsunami, indicating the eddies remained in the port after the leading wave of the tsunami. This suggested that the vessels in the port must pass the entrance until 80 minutes to evacuate outside of the port.

Keywords: Vessel Evacuation, Eddy, the Nankai Trough Earthquake

Numerical experiments on the meteorological tsunami over the East China Sea

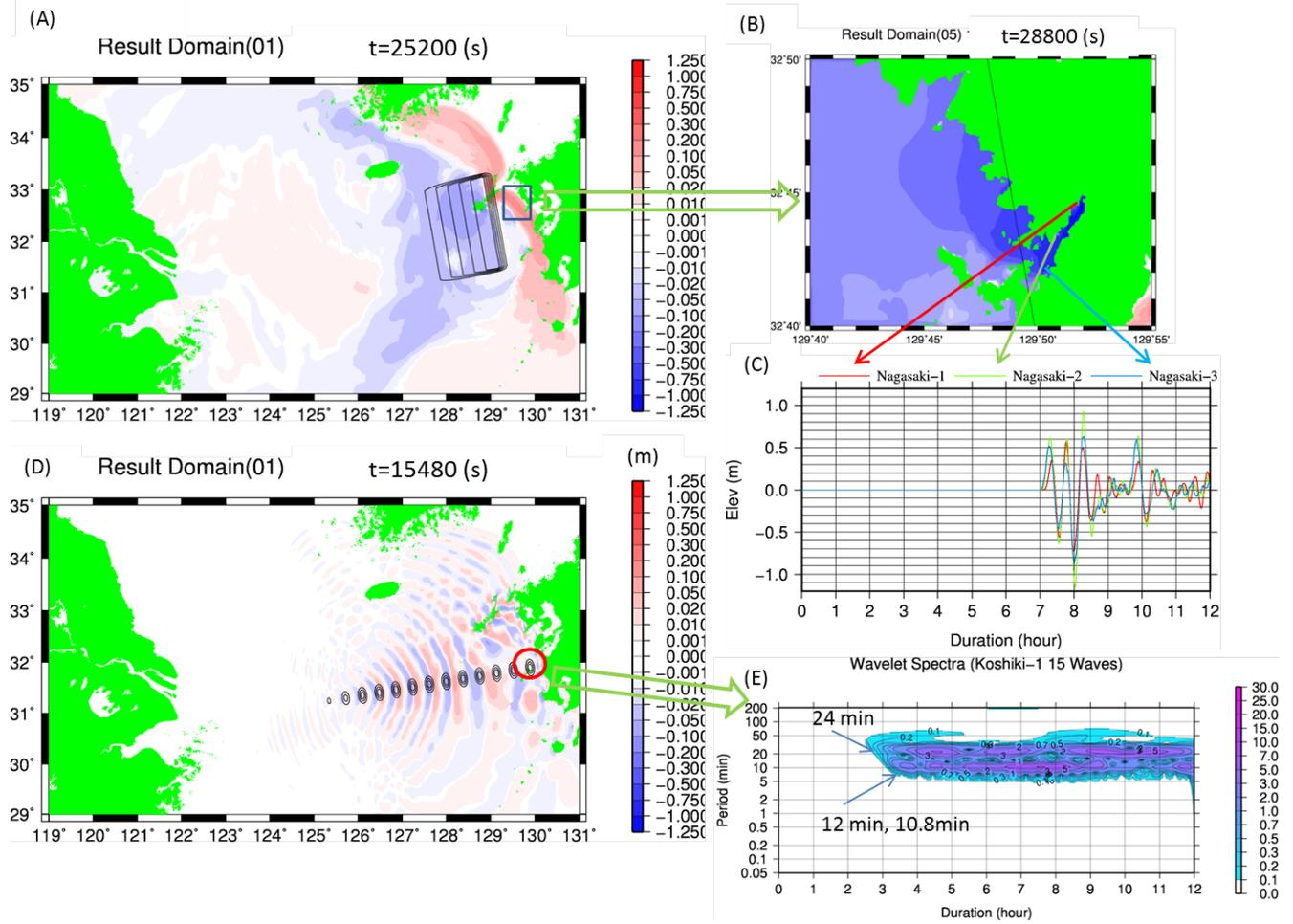
*Kenji Tanaka¹, Daiki Ito²

1.Department of Global Environmental Studies, Hiroshima Institute of Technology, 2.Graduate School of Science and Technology, Hiroshima Institute of Technology

Meteorological tsunami is a kind of ocean long wave with the tsunami frequency band that is driven by atmospheric forcing such as pressure or wind disturbance at the sea interface. The coastal area of west Kyushu, Japan, is one of the regions that often observed the large amplified secondary oscillation higher than 1 m, which seemed to be resulted from meteorological tsunami. The present study is aimed to clarify the propagation and resonant process of the meteotsunami over the East China Sea by numerical experiment.

The multi-nested numerical model was developed with the mainframe of the model based on the Princeton Ocean Model 2008. To smooth the scale-down process, we suggested the blending coefficient, c , as a exponential function to the distance from the boundary of the daughter domain. Two kinds of the pressure disturbance model were examined in the present study. The first model was single triangular wave with the horizontal scale of about 300 km with the +3hPa barometric anomaly. We located such single pressure wave at the coastal area of the east China (121E, 30-33N), and moved to west Kyushu with the speed of 30 m/s. The spilling wave gradually grew ahead of the positive pressure disturbance, and moved much faster than the pressure wave when passing the Okinawa trough. The first spilling wave was reached to the west Kyushu coastal area 30-50 minutes before reaching the pressure wave. In Nagasaki bay, the secondary oscillation became maximized when the wave came from WSW direction (~255T), which was nearly same as the line direction from the mouth to nose of the bay without shadow effect by Goto Island. The maximum amplitude was 2.1 m at the third wave, when the backwash inside the bay overlapped with the inverse pressure effect. The second pressure model was a train of the small pressure waves. The horizontal scale of individual pressure wave was 30-100km and we generated 1-20 waves with the shape of the 2-dimensional Gaussian function. The pressure waves initially located at 31.2N 125E with the period of 20 minutes, moving toward Koshiki Islands, Kagoshima. The maximum intensity of each pressure anomaly was 2.0 hPa. As a result, the ocean long waves were amplified higher than 30 cm and reached to the wide area of west Kyushu. This result implied that the secondary oscillation is possibly amplified even if the pressure disturbance passed more than 100 km away from the harbor. The oscillation sustained for several hours inside the small bay with the mode of eigen oscillation became prevailed instead of the oscillation with the period of the pressure wave.

Keywords: Meteorological tsunami, East China Sea, pressure wave, multi-nested ocean model, resonance



Initial tsunami height estimated by observing tsunami ionospheric hole

*Yuto Tomida¹, Masashi Kamogawa¹, Tatsuya Kanaya¹, Atsushi Toyoda²

1.Department of Physics, Tokyo Gakugei University, 2.Nuclear Safety Research and Development Center, Chubu Electric Power Co., Omaezaki, Japan .

Low frequency acoustic waves, termed infrasonic waves, are excited by sudden displacement of ground and sea surface of mega-scale earthquake (EQ) and tsunami. When the waves reach ionosphere, they disturb the ionospheric plasma. The plasma variation has been detected by measurement of total electron contents (TEC) between a satellite of Global Positioning Systems (GPS) and a receiver on the ground. In addition to the waves, a TEC depression lasting for a few minutes to tens of minutes also occurred above the tsunami source area, termed tsunami ionospheric hole (TIH), in the mega-scale EQ with tsunami. The largest of the TEC depression appeared 10 to 20 minutes after the main shock. In this paper, we show the quantitative relation between an initial tsunami height and a depression rate of TEC caused by the TIH. Accordingly, the ionospheric TEC measurement is applicable to an early warning system of tsunami, when it takes more than 20 minutes for the tsunami to arrive coastal area.

Keywords: Ionospheric hole , Inland earthquake, Tsunami

Heights of the Tsunamis of the 1946 Showa-Nankai and the 1960 Chilean Earthquakes on the West Coast of Wakayama Pref.

*Takashi Yanuma¹, Yoshinobu Tsuji², Hiroshi Kadota¹, Masami Sato³, Yayoi Haga³, Fumihiko Imamura³

1.PASCO Corporation, 2.Fukada Geolog. Inst., 3.IRIDeS, Tohoku Univ.

The 1960 Chilean tsunami was observed along the wide coastal area of Pacific Ocean from Hokkaido through Okinawa. The tsunami was also observed at the coast of Wakayama prefecture. The dense explorations were done east of Susami town, but few explorations were done at the west coast of Wakayama prefecture (from Wakayama city through Kushimoto town). About 1960 Chilean tsunami, we can find the records in the newspapers at the day of the arrival and municipal bulletins. We surveyed these records for getting the precise records of the 1960 Chilean tsunami.

In this exploration, we also surveyed the records of 1946 Showa-Nankai earthquake tsunami that caused big damage to Wakayama prefecture. Various investigations were undertaken. In "Showa Kii Koro-no ki" (1948), a report on this earthquake, the situations of the inundation of the tsunami on the coastal villages and the reports from municipal offices and schools are described, but surveys were not taken. So, we found out the present position of inundation point from the figures in the report and measured the precise position and height.

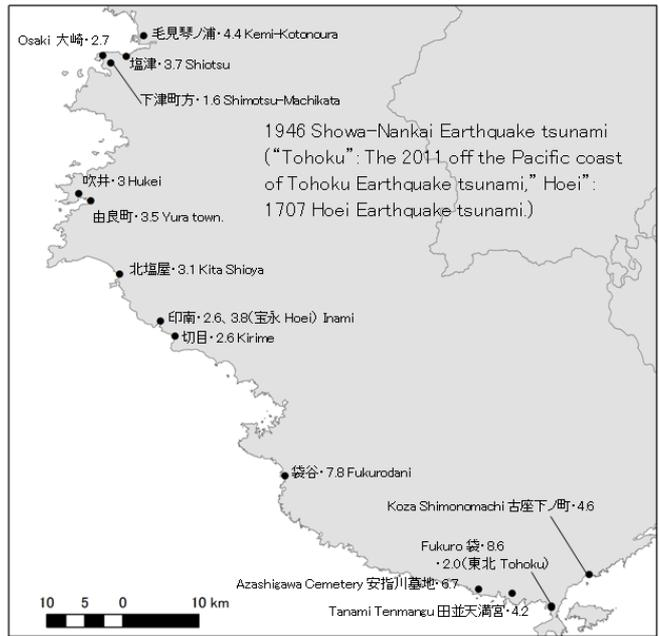
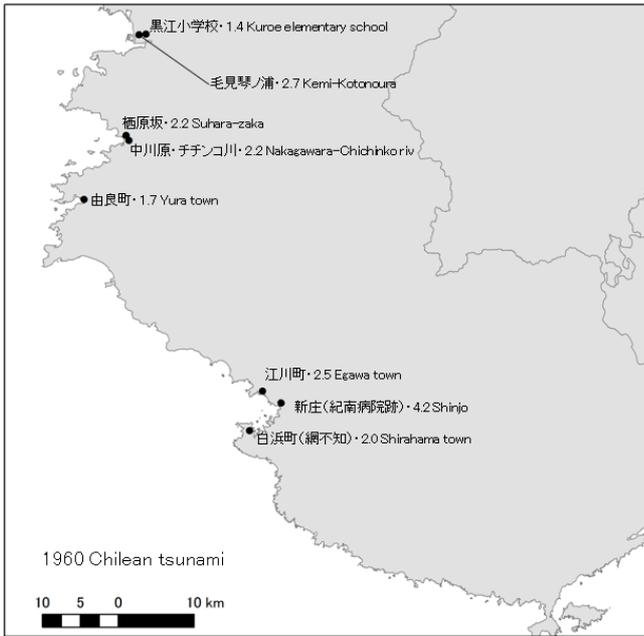
During the exploration, we did interviews about these tsunamis from the habitants who lived along the coast. We also interviewed about 2011 off the Pacific coast of Tohoku Earthquake, and we did surveys if we could get the exact point of inundation.

The exploration was carried out from 14th of January of 2015 to 16th of January. About 1960 Chilean tsunami, we could obtain the following surveying results of tsunami height; Kemi-Kotonoura, wakayama city, 2.7m, Kuroe elementary school, Kainan city, 1.4m, Suharazaka, Yuasa city, 2.2m, Nakagawara Chichinko river, 2.2m, Yura town, Ajiro, 1.7m, Egawa town, Tanabe city, 2.5m, remained state of Kinan hospital, 4.2m, Tsuna-shirau, Sirahama town, 2.0m. As 1946 Showa-Nankai earthquake tsunami, we could obtain 1.6 -8.6m of tsunami height. Especially, by interviewing the local information, we could obtain the tsunami height of 7.8m at Fukurodani of Shirahama town and 6.7m at Azashigawa cemetery. In addition to the record of 1946 Showa-Nankai earthquake tsunami, we could obtain the record of 1707 Hiei earthquake tsunami at the Injoji temple of Inami, and the tsunami height of 3.8m was measured.

About the tsunami of the 2011 off the Pacific coast of Tohoku Earthquake, we could hear from the habitants that they felt nothing or only the quaking of sea surface. But the inundation was observed at Fukuro, kushimoto town, and we could get the tsunami height of 2.0m.

Part of this study was carried out in the commissioned project of Nuclear Regulation Authority.

Keywords: the 1960 Chilean tsunami, the 1946 Showa-Nankai earthquake tsunami, Wakayama Prefecture, Kii Peninsula



Height Distribution of the Tsunami of the South Kanto Earthquake of February 3rd, 1605

*Yoshinobu Tsuji¹

1.Fukada Geolog. Inst.

In the midnight of February 3rd, 1605, a large earthquake occurred in the south sea area of Honshu, Japan. Accompanied with this earthquake a huge tsunami was generated, and large damage took place on the coasts of Boso peninsula, and of Shikoku Island. This earthquake was considered as an Tokai-Nankai gigantic earthquake, or the twin earthquake consists of the source areas of Nankai and south Kanto Sea region. Large tsunami heights were recorded at the coasts of Hachijo-island, Boso peninsula, and Tokushima and Kochi prefectures, Shikoku. But, old document records of this tsunami were poor on the coast of Tokai district and Kii peninsula, and moreover earthquake shaking was not felt at Kyoto, the capital of Japan in those years. These facts suggests that the source area of this earthquake was not extended to the Tokai Sea area. Ishibashi & Harada(2013) proposed that the source of this earthquake is possible to be situated at Ogasawara trench area.

The damage of this earthquake tsunami is mentioned in the text of a "Boso Chiran-ki" ("the Chronological story of battles in Boso Peninsula"), in which 35 names of tsunami damaged villages were listed. The author was informed from a priest of the temple "Saitokuji" in Amazura village, which is one of the listed village. He showed me that several old documents were kept in this temple, and the main image of God was carried by the tsunami. I measured the level of the location of the main god and clarified that the tsunami height was 17.3m at this temple. On the other hand we collected detailed map in the scale of 2,500 to 1 for the damaged coastal villages. I checked the lowest height (above mean sea level, MSL) of each damaged village, and found out the lowest values of the inundated height can be estimated at five villages. Fig 1 shows the residential area of Yasashido village, and the lowest height of the ground of the houses is 7.7m above MSL, which shows sea water rose up to 9.7 meters there, because Koshimura(2002) showed that a house will be entirely collapsed in the case the thickness of water over 2.0 meters. We finally obtained the distribution of (the minimum estimated) tsunami heights as Fig 2.

Keywords: The 1605 Keicho south Kanto Earthquake-Tsunami, Boso peninsula, old documents kept in a temple

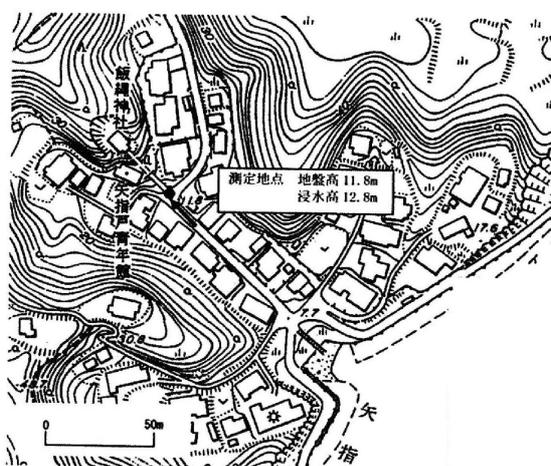


図1 千葉県いすみ市大原字矢指戸の2,500分の一住宅地図

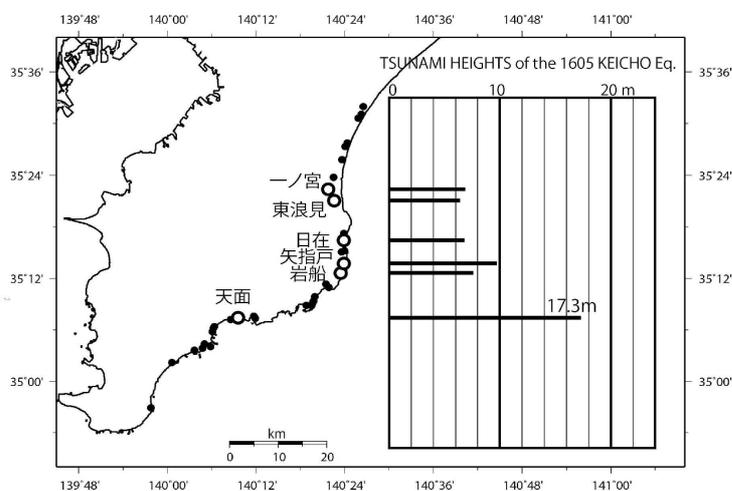


図2 『房総治乱記』に記載の35ヶ村(丸印)。白丸は津波浸水高さを推定しうる村で、右グラフは推定津波浸水高

Modeling of the 1703 Genroku Kanto earthquake tsunami based on historical documents in Choshi City, Chiba prefecture

*Hideaki Yanagisawa¹, Yoshifumi Takamori², Kazuhisa Goto³, Kaito Suzuki¹

1.Department of regional Management, Faculty of Liberal Arts, Tohoku Gakuin University, 2.Choshi Municipal Choshi High School, 3. International Research Institute of Disaster Science, Tohoku University

The 1703 Genroku Kanto earthquake and tsunami caused catastrophic disaster in Kanto region. According to the previous studies, the modeling of the 1703 earthquake is mainly performed by the inversion analysis from observed fault deformations on land. However, it is difficult to model an offshore fault along the Sagami trough from land deformations because an offshore fault has an insignificant effect on land deformations. Thus, it is important to consider historical tsunami data to model the 1703 Genroku Kanto earthquake. We study the tsunami heights focusing on historical documents in Choshi city which locates at eastern edge of the Kanto region. There are three historical documents for the 1703 Genroku Kanto earthquake tsunami: 1) Tanaka Genba Sendaisyu kan no maki 2) the historical document of the Homan temple 3) the historical document of the Tokai shrine. Based on these documents, we estimated the tsunami heights of T.P. 5.9 m, T.P.11.7m, T.P. 7.7 m, T.P. 10.8 m, T.P. 4.8 m in Iseji, Kobatake-ike, Nagasaki, Tokawa and Na-arai, respectively. Although tsunami heights have been assumed from 0.9 m to 4.0 m in Choshi in previous studies, we found that the significant tsunami with more than 10 m attacked Choshi area. We further study the fault model of the 1703 Genroku Kanto earthquake using new data of the tsunami heights in Choshi. We first confirmed whether the previous models (Cabinet Office, 2013; Namegaya et al., 2011; Satake et al., 2008 (ShishikuraABC)) can reproduce the inundation of Kobatake-ike pond where reliable descriptions are in historical documents. As results, we found that previous models cannot inundate Kobatake-ike area. To reproduce the tsunami heights in Choshi, we modified the fault model with extending the fault length along Sagami trough. Consequently, the fault model with more than 120 km fault length along Sagami trough can inundate Kobatake-ike area. From this result, we estimated that the fault of the 1703 Genroku Kanto earthquake could rupture about 120 km offshore along Sagami trough. A future study will be to provide detailed fault model with more evidence other than Choshi area.

Keywords: The Genroku Kanto earthquake tsunami, Historical document, Numerical simulation, Fault model, Choshi city, Chiba prefecture

Identification of dominant phases as reflected waves in tsunami observed on Pacific Ocean-Application to the 2011 Tohoku Tsunami

*Kuniaki Abe¹, Masami Okada², Yutaka Hayashi²

1.none, 2.MRI

Abstract

Reflectors of tsunami are assumed in the Pacific Ocean and the travel times are calculated on refraction diagrams of the reflected waves in order to explain dominant phases as reflected waves in the following waves of tsunami. The travel times are compared with travel times of large-amplitude phases observed at tide stations and the phase is identified as the reflected wave from the consistency of travel time. The work is repeated for 21 assumed reflectors in the Pacific Ocean. This method was applied to the 2011 Tohoku tsunami. Starting times of the reflected wave were determined from the arrival times of large positive phases in tide gauge records in the neighborhood of the reflector. One to four arrival times between first and maximum waves are considered as possible origin times of reflected waves. Reflected waves from all the assumed reflectors were compared for all the arrival times of dominant phase. The reflected waves were identified for large-amplitude phases recorded at fifteen stations all over the Pacific. As the result almost all the dominant phases were identified as reflected waves from the assumed reflectors. Totally 118 answers of the reflect waves were obtained having the standard deviation of 0.52 hr. The identification of dominant phases as reflected waves recorded in Japan is show in Fig.1.

Keywords: 2011Tohoku Tsunami , Tide gauge records, Pacific Ocean, Reflected Waves, Reflectors

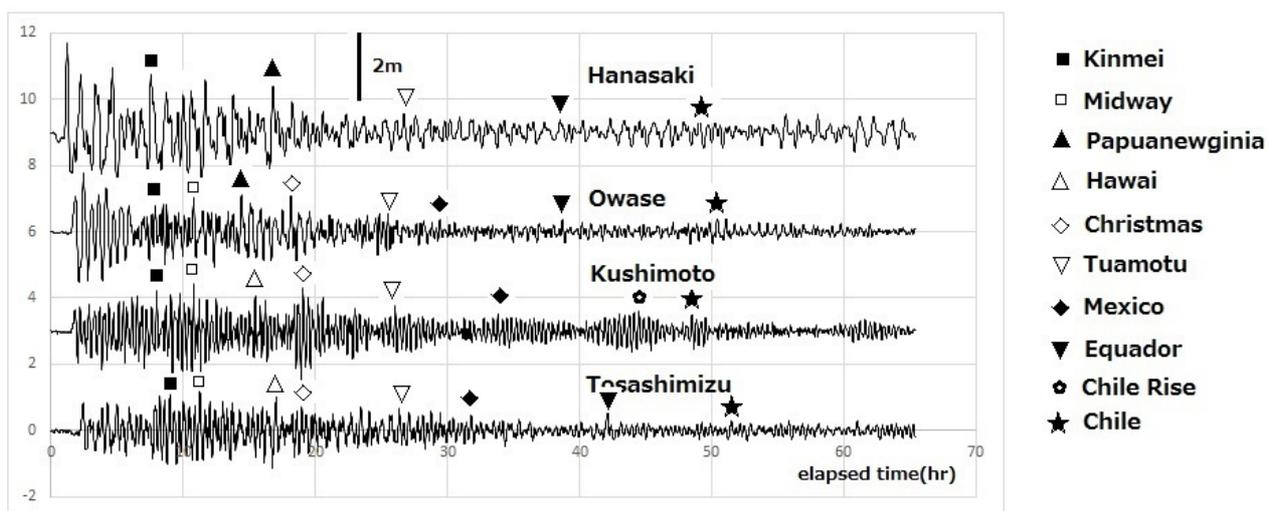


Fig.1

Slip Distribution of the November 2006 and January 2007 Kuril Earthquakes from Inversion of Phase-corrected Tsunami Waveforms

Toshiki Doyama¹, Satoshi Kusumoto¹, Shingo Watada¹, *Kenji Satake¹, Yushiro Fujii²

1.Earthquake Research Institute, The University of Tokyo, 2.Building Research Institute

Along the Kuril-Kamchatka trench, two Mw 8-class earthquakes occurred at a two-month interval: an intraplate underthrust earthquake in November 2006 (Mw 8.3, the Global Centroid-Moment-Tensor (CMT) Project) and an outer-rise normal fault earthquake in January 2007 (Mw 8.1, the Global CMT Project). Tsunamis generated by the two earthquakes were recorded at far-field observation stations in Hawaii (e.g. Hilo) and the west coast of the United States (e.g. Crescent City) as well as in and near Japan and Russia.

We usually forecast and invert tsunami waveforms by assuming the linear long waves. However, we could not use far-field tsunami waveforms for inversion because simulated tsunamis arrive earlier than observed ones, and the initial phases of simulated and observed ones show the reverse polarity at far-field stations. Recently, Watada *et al.* (2014) completely explained the observed tsunami delay and developed a model to correct the initial phases of synthetic waveforms. In this study, we estimated the fault slip distribution of the two earthquakes from tsunami waveform inversion using the tsunami phase correction method (Watada *et al.*, 2014).

The slip distribution of the November 2006 Kuril earthquake estimated by using phase-corrected tsunami waveforms indicates that a main rupture area is located in the shallower side, which is different from the slip distribution estimated by using uncorrected tsunami waveforms (e.g. Fujii and Satake, 2008), where the deeper side has a large slip amount, and agrees well with the inversion results of previous studies estimated from teleseismic body waves (e.g. Lay *et al.*, 2009). For the January 2007 Kuril earthquake, the location of a main rupture area estimated by using phase-corrected tsunami waveforms also approximately coincides with the inversion results of previous studies estimated from teleseismic body waves. At far-field observation stations as well as at near-field observation stations, the phase-corrected synthetic waveforms agree very well with the observed waveforms. Furthermore, by using phase-corrected tsunami waveforms for inversion, the seismic moment and moment magnitude become larger and closer to the Global CMT solution and previous inversion results estimated from teleseismic body waves. Therefore, through the tsunami phase correction method, far-field tsunami waveforms can be used for the inversion for the slip distribution estimation.

Keywords: Kuril earthquakes, Kuril-Kamchatka trench, Fault slip distribution, Tsunami waveform inversion, Tsunami phase correction method, Far-field observation stations

2015 Torishima tsunami earthquake: Tsunami observation at short distances by an array of ocean bottom pressure gauges

*Yoshio Fukao¹, Hiroko Sugioka², Aki Ito³, Hajime Shiobara⁴, Osamu Sandanbata⁴, Shingo Watada⁴, Kenji Satake⁴

1.CEAT/JAMSTEC, 2.Science/Kobe Univ., 3.D-EARTH/JAMSTEC, 4.ERI/Univ. Tokyo

The 2015 May 02 Torishima earthquake generated tsunamis with heights as large as 60 cm at Hachijo Island, 180km to the north of the epicenter, yet the seismic magnitude was only 5.7 and there was no report of seismic intensity of 1 or more. The earthquake can be regarded as a tsunami earthquake. The epicenter is located closely near the Smith Caldera and the focal mechanism is of CLVD-type. The seismic and tsunami waves were recorded by our pressure gauge array deployed at the bottom of the open sea about 100km to the NNE from the epicenter. Here we report the results of our observation.

(1)The array consists of 10 ocean bottom pressure gauges using ParoScientific quartz resonators which can measure absolute water pressure at 7000m depth with nano-resolution. The array configures equilateral triangles with minimum and maximum lengths of 10 and 30km, which was in operation for a year from May 2014 to May 2015. Sampling rate was set at 4Hz, with which the response to pressure disturbance is almost flat below 0.2Hz.

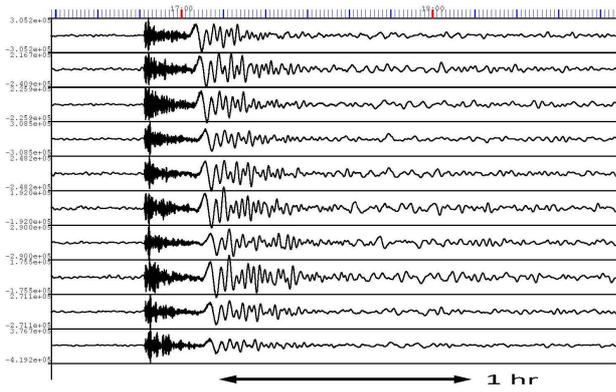
(2)The tsunami trace at each site starts with positive onset (pressure increase) and reaches a maximum amplitude of about 200Pa (\approx 2cm in tsunami height). Records of ordinary thrust earthquakes with similar magnitudes at similar epicentral distances show comparative amplitudes of seismic waves but no visible tsunamis (Fig.1).

(3)Tsunami slowness vector is measured under the plane wave approximation. The measured slowness varies as a function of frequency in a consistent way with the linear dispersion theory. The slowness vector orientation deviates clearly from the great circle path and changes slowly as a function of frequency as expected from the frequency-dependent ray tracing (Sandnabata et al., 2016, JpGU). This ray tracing also demonstrates strong ray focusing towards Hachijo Island and no such focusing towards the array, explaining qualitatively the marked contrast in tsunami height between the array (\sim 2cm) and Hachijo Island (\sim 60cm).

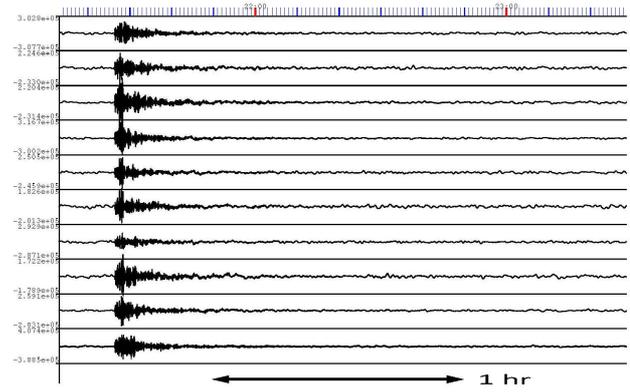
(4)The tsunami spectrum at each station shows consistently a broad peak around 3.5mHz and sharp double peaks around 8mHz. We interpret the first broad peak as due to the primary tsunami source associated with seafloor uplifting and the sharp double peaks as due to wave resonance inside the Smith Caldera.

Keywords: tsunami earthquake, tsunami observation, water pressure gauge

**A: 2015 Tsunami earthquake
M5.7 Depth 12km**



**B: 2015 Near-trench thrust earthquake
M5.6 Depth 18km**



2015 Torishima tsunami earthquake: Ray tracing analysis of dispersive tsunami wave

*Osamu Sandanbata¹, Shingo Watada¹, Kenji Satake¹, Yoshio Fukao², Hiroko Sugioka³, Aki Ito², Hajime Shiobara¹

1.Earthquake Research Institute, the University of Tokyo, 2.Japan Agency for Marine-Earth Science Technology, 3.Department of Planetology, Kobe University

On 3 May 2015 (JST), an M5.7 earthquake occurred near Torishima Island and generated abnormally larger tsunami, compared to its magnitude, with heights as large as 60 cm at Hachijo Island, 180 km to the north of the epicenter. This earthquake may be regarded as a tsunami earthquake. The earthquake source is located at the shallow part near the Smith caldera, a volcanic body on the shallow ridge along the Izu-Bonin trench, where three similar earthquakes occurred in 1984, 1996 and 2006 (Satake and Gusman, 2015, SSJ). For the 1984 earthquake, Satake and Kanamori (1991, JGR) simulated tsunami propagation using the linear long-wave theory and suggested the tsunami source may be explained by a circle-shaped uplift of sea surface. The focal mechanism was explained by CLVD-type models due to volcanic activity in the shallow part, such as hydrofracture associated with magma injection (Kanamori et al., 1993, JGR) or a seismic slip on curved, cone-shaped faults (Ekström, 1994, EPSL).

Tsunami waves caused by the 2015 earthquake were recorded by a temporary ocean bottom array of water pressure gauges, 100 km to the NNE from the epicenter. The tsunami traces at the array gauges started with a positive onset and showed dispersion effects. It is notable that the measured slowness orientation of wavefront approximated by a plane wave varies as a function of frequency (Fukao et al., 2016, JpGU).

In this study, we investigated frequency-dependent ray paths of the tsunami by a ray tracing method considering the dispersion effects. We first iteratively calculated two-dimensional phase- and group-velocity fields dependent on frequency, using the theoretical formula of gravity waves and a smoothed bathymetry. These velocity fields enable us to measure travel times of both of wavefronts and wave packets. We assumed a tsunami source on the Smith caldera and applied the ray equations for seismic surface waves on spherical Earth (e.g. Sobel and Seggern, 1978, BSSA; Jobert and Jobert, 1983, GRL) to ray tracing of tsunamis.

Ray paths show that longer-period waves are more affected by bathymetry variations. We note that wavefronts toward NNE at the source change their direction to the north, furthermore to the NNW in case of longer-period waves. This trend explains well the frequency-dependent slowness orientation of wavefront at the array gauges. Travel times of wave packets are also consistent with frequency-dependent arrival times observed at the gauges. In addition, ray paths show an intensity of energy northward along the shallow ridge, regardless of frequency, which might have contributed to high amplitudes at Hachijo Island.

Our ray tracing method including dispersion effects allows us to investigate ray paths for shorter waves out of applicable range of the linear long-wave theory. Therefore we can consider path effects for shorter waves following primary longer waves. This method may be also applicable for tsunami forecasting including subsequent shorter waves due to dispersive effects with small numerical computation costs.

Keywords: tsunami, dispersion, tsunami earthquake, ray tracing, volcanic earthquake

An improvement of the antenna installation mechanism for satellite communication of the GPS tsunami meter

*Yukihiro Terada¹, Sin'ichi Yamamoto², Naohiko Iwakiri², Tadahiro Iwasaki³, Naokiyo Koshikawa³, Mitsuo Tada⁴, Akira Wada⁵, Teruyuki Kato⁶

1.Kochi College, National Institute of Technology, 2.National Institute of Information and Communications Technology, 3.Japan Aerospace Exploration Agency, 4.Yuge College, National Institute of Technology, 5.Hitachi Zosen Corporation, 6.Earthquake Research Institute, The University of Tokyo

The tsunami observation system using GPS buoys succeeded to detect 11th March 2011 Tohoku-Oki earthquake tsunami. Through this experience, we recognized the problems to be solved. One of these problems is that the real-time monitoring of the tsunami data stopped suddenly after the highest wave was observed. Since the data of all GPS buoys installed in this area stopped at once, it was thought that the cause was interception of the communication network by electric power loss. Then, a satellite data transmission will be the solution. If satellite data transmission is possible, the data have not to be sent to the area nearest to the coast, which allows us that the data can be safely recorded without interruptions due to earthquakes and/or tsunamis. The Japanese engineering test satellite (ETS-VIII) was used for the purpose of data transmission. The data that was obtained on the buoy was transmitted to the land base and was shown on a webpage in real-time, successfully.

However, the data transmission capability is still a problem as it varies depending on the wave height. As we used a planer antenna for single transmission and acquisition, it has a directional property depending on zenith angle. If the buoy inclines larger, the gain of signal gets lower and the frame error rate increases. The antenna installation mechanism for making this change small was made as an experiment, and a small change compared with the fixed mechanism. As the effective function having been checked by this experiment, a practical apparatus is due to be taken. The experiment was supported the budget of the head of Earthquake Research Institute of the University of Tokyo.

Keywords: GPS tsunami meter, ETS-VIII, satellite data transmission

Tsunami alarm equipment (3)

*Akio Katsumata¹, Yutaka Hayashi¹, Kazuki Miyaoka¹, Hiroaki Tsushima¹, Toshitaka Baba²

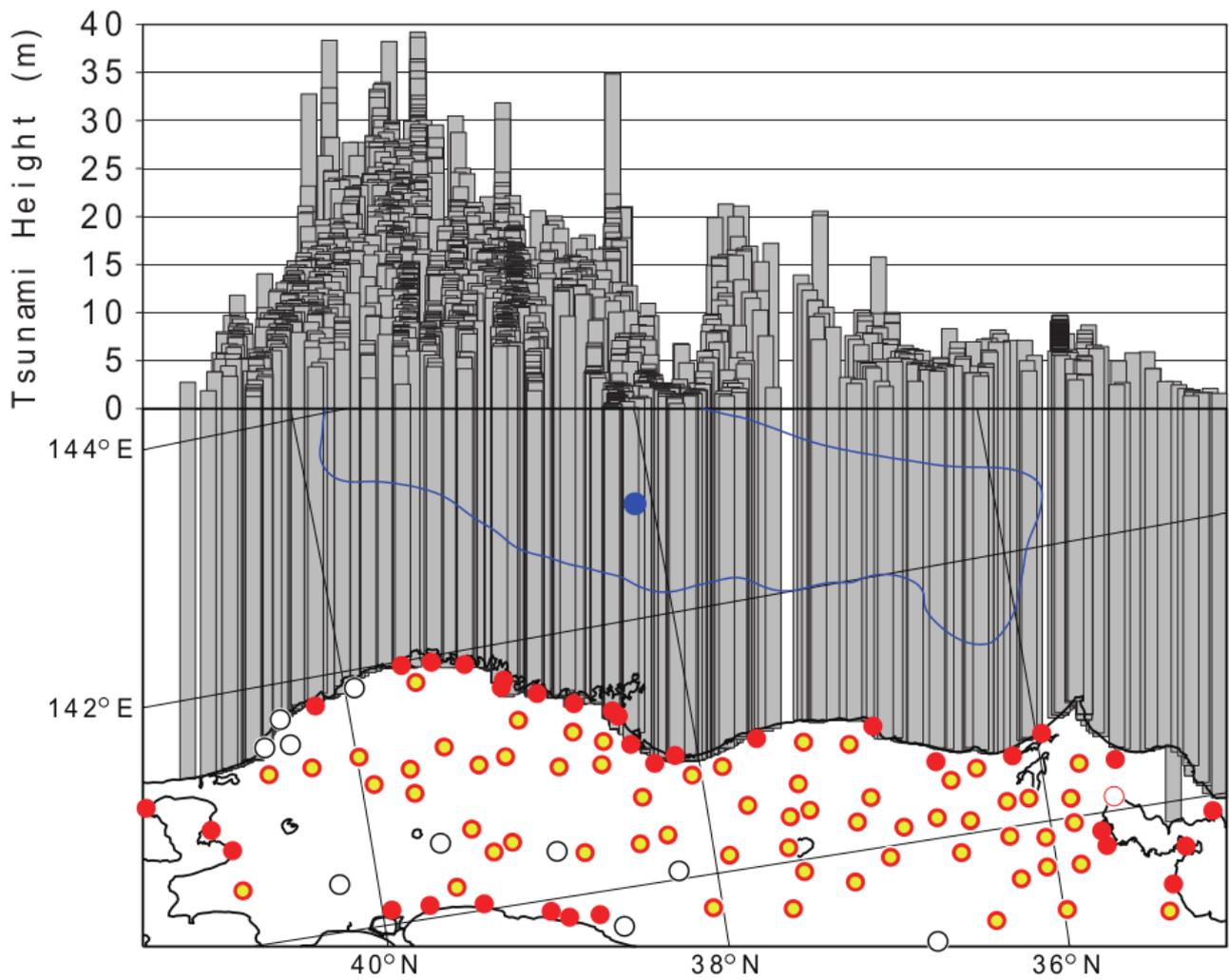
1.Meteorological Research Institute, Japan Meteorological Agency, 2.Tokushima University

We investigated possibility of appliance to alarm tsunami hazard from single site ground motion observation. It is considered that one of the quickest ways of tsunami evacuation is transfer to higher place soon after a strong and long ground shaking. Strong ground motion means that the source area of the event would be close to the current location, and long ground shake or large displacement mean that the event magnitude would be large.

At the first, we limited epicentral distance by setting upper limit of the modified Mercalli seismic intensity of 5.5, which is obtained by converting peak ground velocity. The seismic intensity corresponds to epicentral distance of about 140 km for an earthquake of Mw 8.0. We tried to find a threshold instrumentally observable value which distinguishes earthquakes with tsunami potential from others. Thread score is used to obtain the optimal threshold value. It was found that a suitable value for single site tsunami alarm would be strong-motion duration of long-period peak displacement. Although two threshold magnitude of 7.8 and 8.5 were tried, clear difference was not recognized in the score.

Applying this method to recent major earthquakes, it was shown that this method is partly effective to inform possibility of disastrous tsunami. When the source area is away from the shoreline, such as northern area of the 2011 off the Pacific coast of Tohoku Earthquake, the observed values were lower than the threshold. We expect this method would work as complimentary alarm for evacuation from tsunami.

Keywords: tsunami alarm, instrumental seismic intensity, single station processing



Was the submarine landslide which caused the 1998 Papua New Guinea tsunami detectable by a seismograph?

*Akio Katsumata¹, Kenji Nakata¹, Kenichi Fujita¹, Masayuki Tanaka¹, Akio Kobayashi¹, Yasuhiro Yoshida²

1.Meteorological Research Institute, Japan Meteorological Agency, 2.Meteorological College, Japan Meteorological Agency

The 1988 Papua New Guinea tsunami caused casualties over 2,200 (Tappin 2008). The tsunami higher than 10 m followed an earthquake of Mw 7.0. It is considered that the tsunami was caused by a submarine landslide because the tsunami was higher than that expected for an earthquake of magnitude 7, the tsunami generation was estimated about 10 minutes after the earthquake, and submarine topography which seemed to have been related to the landslide was identified (e.g., Tappin et al., 1999). Tsunami caused by an ordinary earthquake can be aware of before its arrival by seismic analysis. In the case of the 1988 Papua New Guinea tsunami, it was impossible to prepare for the tsunami only by the ordinary seismic analysis. Here we discuss possibility of detecting landslides with seismic method.

Watts et al. (2003) estimated the landslide which could caused the 1998 tsunami at the length of 4.5km, the width of 5km, and the thickness of 760m. The mass was considered to have slumped on a slope of 12 degree dip with characteristic time of 32 seconds. The force causing the landslide was gravity. The friction and drag of water decelerated the mass. It is considered that the mass was being held with the static friction, and it dropped to dynamic friction when the mass started to slide. The ground was considered to be subject to the force change between the static and dynamic frictions.

The force is estimated at

$$(\rho_1 - \rho_2)Va,$$

where ρ_1 is the density of the ground mass ($2.15 \times 10^3 \text{ kg/m}^3$), ρ_2 the density of the water ($1.0 \times 10^3 \text{ kg/m}^3$), V volume of the mass ($4,500 \text{ m} \times 5,000 \text{ m} \times 760 \text{ m}$), a the initial acceleration (0.36 m/s^2). It turn out to be $7 \times 10^{12} \text{ N}$. The force by the collapse of Mt. Saint Helens in 1980 was estimated at $2.6 \times 10^{12} \text{ N}$ (Kanamori et al., 1984). The force by the drain-back at Mt. Mihara in Izu-Oshima in 1987 was estimated at $4 \times 10^{11} \text{ N}$ (Takeo, 1990). For the case of the Papua New Guinea event, similar order of force could act on the ground. If a single force of $7 \times 10^{12} \text{ N}$ and source time duration of 30 seconds was applied, it is expected that some seismic records would have been recognized at PMG station (900 km from the event) under a condition of no other seismic source. However the seismic wave by the earthquake was larger than the expected amplitude, and no clear long-period trace was recognized on the seismic record.

Keywords: tsunami by landslide, seismic record, 1998 Papua New Guinea tsunami

Landslide model of the 1741 Oshima-Oshima eruption

*Kei Ioki^{1,2}, Yuichiro Tanioka¹, Gentaro Kawakami³, Yoshihiro Kase³, Kenji Nishina³, Wataru Hirose³, Satoshi Ishimaru³, Hideaki Yanagisawa⁴

1.Institute of Seismology and Volcanology, Hokkaido University, 2.National Institute of Advanced Industrial Science and Technology, 3.Geological Survey of Hokkaido, 4.Department of Regional Management, Faculty of Liberal Arts, Tohoku-gakuin University

The 1741 tsunami occurred near Oshima-Oshima in Hokkaido caused great damage along the coast of Japan Sea in Oshima and Tsugaru peninsula. Assuming that the tsunami was generated by flowing a landslide into the sea with a sector collapse in Oshima-Oshima, the landslide was simulated. Distribution of debris deposits, topography before the sector collapse, and landslide volume were re-calculated from a bathymetry survey data (Satake and Kato, 2001) in the north part of Oshima-Oshima. Based on these data, the landslide was simulated using the integrated model of landslide and tsunami (Yanagisawa et al., 2014). As a result, distribution of computed debris deposits agree relatively well with the distribution of debris deposits made out from bathymetry. However, the computed debris deposits spread to north part than debris deposits made out from bathymetry and not reach to the east and west part compared to debris deposits made out from bathymetry in detail. The thickness of computed debris deposits was thicker to the north part than debris deposits made out from bathymetry. Further, model parameters and topography before the sector collapse are needed to be improved for more realistic tsunami simulation.

Keywords: landslide, tsunami, Oshima-Oshima

Re-estimation of damages in the Miyako District Okinawa by 1771 Great Meiwa Tsunami

*Takeshi Matsumoto¹

1.Faculty of Science, University of the Ryukyus

Precise description of damages by devastating 1771 Great Meiwa Tsunami (Yaeyama Earthquake Tsunami) is recorded in "Kyuyo", the chronicle of the Ryukyu Dynasty and "Otoiai-gaki", local manuscript in Miyako district. Run-up heights at several villages in Miyako District recorded in this manuscript were compared with the result of the recent Tsunami Height Assessment in Okinawa Prefecture (released in 2015). Most of the recorded run-up heights were smaller than the recent assessment assumed by 8m slip of the three major faults along the southwestern Ryukyu Trench off Yaeyama and Miyako districts. The difference may cause the difference in slip rate along the faults and the slip rate might be smaller off Miyako than that off Yaeyama. Another possibility may be that a rupture along the fault plane was generated off Yaeyama and propagated towards Miyako where it terminated.

Keywords: Great Meiwa Tsunami, run-up height, Miyako District

Accurate measurement of the tsunami heights of the Kanpo Tsunami of 1741 caused by the volcanic eruption of Oshima-Ooshima Island on the coasts of Esashi and Matsumae districts, Hokkaido

*Yoshinobu Tsuji¹, Yosuke Kuroyanagi², Yuya Narita², Takahiro Kinami³, Mutsumi Shiraishi⁴, Masami Sato⁵, Yayoi Haga⁵, Fumihiko Imamura⁵

1.Fukada Geological Institute, 2.Pacific Consultants Co. Ltd., 3.Kubiki Technology Co. Ltd., 4.Kita-Nihon Historical Disaster Institute, 5.IRIDEs, Tohoku Univ.

In the early morning of August 28th, 1741, Oshima-Ooshima volcanic island, off the coast of SW Hokkaido became active, and a huge tsunami was generated. The tsunami hit the coasts of Matsumae and Esashi districts, Hokkaido. Height distribution of this tsunami had been studied by Harori(1984), Imamura et al(1998), and Tsuji et al(2002). In the present study, tsunami height estimation was made by several newly developed ways. We checked the numbers of damaged houses, casualties, and wrecked ships for each coastal village. On the other hand we researched total numbers of houses and population for each coastal village. We calculated the percentage of damaged houses to total number, and of casualties to the population. We decided the point of ground height measurement with considering the percentage of damage. For the case of villages where almost all houses were swept away, we measure the ground height at the highest point of the residential area of the village. In each village on the coast of Matsumae and Esashi districts of Hokkaido, a shrine had been generally situated behind the highest point of the residential area of the village. Some villages has such historical record that "Whole the houses in this villages were entirely swept away, but only shrine was safe". For such villages, we measured the ground height between the house on the highest ground and the shrine.

Our field surveys were made during 14th to 16th December, 2015 on Hokkaido coast. Fig. 1 shows the result of tsunami height distribution. White circles on the coast show the measured points with high reliability, and black circles show that with less accuracy or reliability.

Acknowledgement: The present study was achieved as a part of the commissioned research named "Study on the historical tsunamis in Japan Sea (2015)" on disaster prevention for nuclear facilities proposed by the Nuclear Regulation Authority, Japan.

Keywords: tsunami caused by a volcanic eruption, accurate measurement of height of a tsunami, the tsunami generated by the 1741 Oshima-Ooshima volcanic eruption

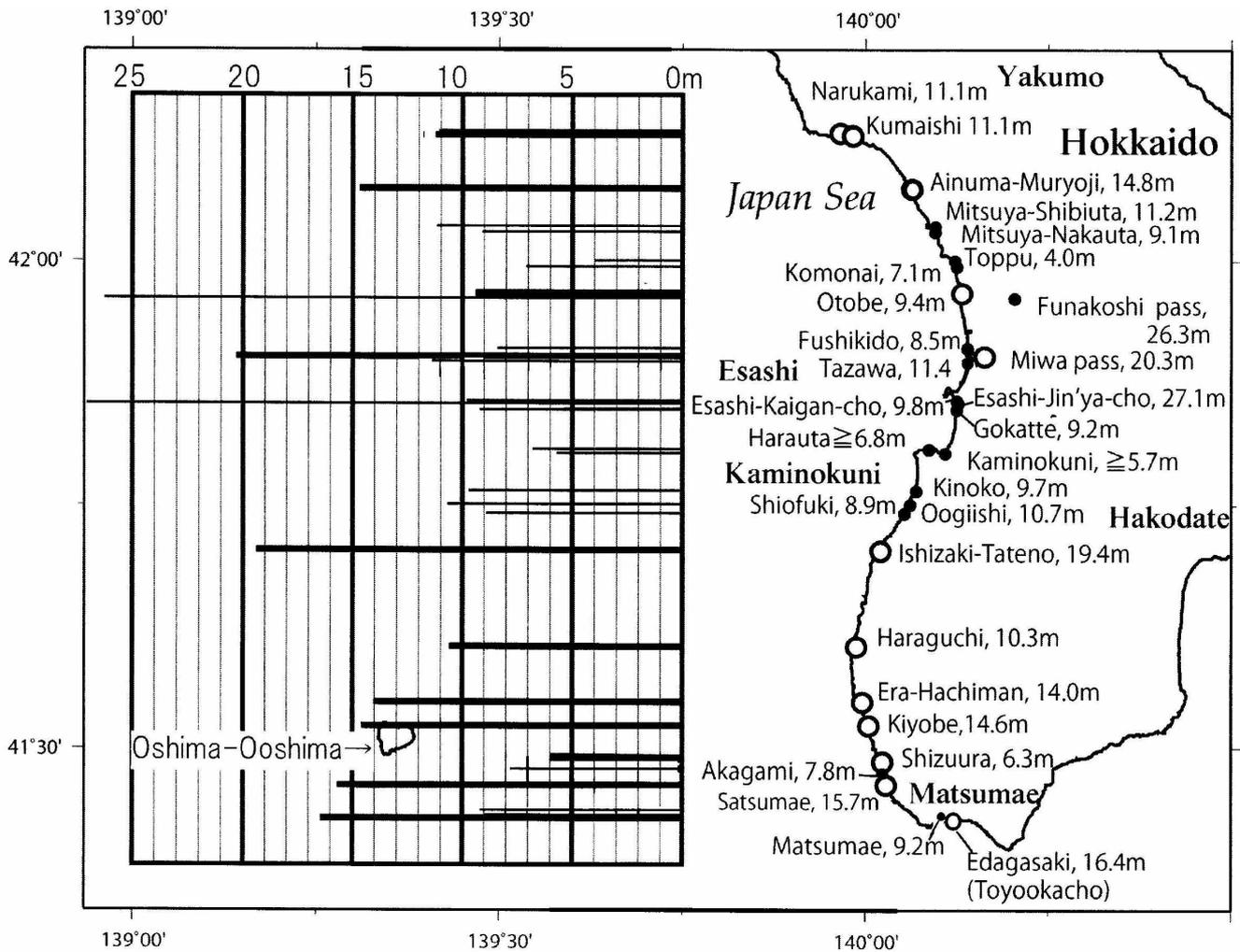


Fig. 1 Height Distribution of the tsunami caused by the volcanic eruption of Oshima-Ooshima in 1741.

Tsunami heights of historical tsunamis based on the "Japan Tsunami Trace database" and other tsunami trace data along the Pacific Coast of Iwate Prefecture

*Keita Takada¹, Hidenori Shibata², Atsushi Odashima², Kentaro Imai³, Yuichi Ebina⁴, Kazuhisa Goto⁴, Shin Koshiya⁵, Hidekazu Yamamoto⁵, Masanobu Shishikura⁶, Atsuo Igarashi¹, Toshihiko Ichihara¹, Hirohisa Kinoshita¹, Tetsuya Ikeda¹

1.Fukken Co.,Ltd., 2.River Division,Department of prefectural Land Development,Iwate Pref Govt, 3.JAMSTEC, 4.IRIDEs Tohoku University, 5.Faculty of Engineering, Iwate University, 6.Institute of Earthquake and Volcano Geology, AIST

Iwate Prefecture is advancing examination for future tsunami hazard based on scientific knowledge such as historical records and tsunami deposits. We referred to the "Japan Tsunami Trace database" and previous studies about tsunami heights and arranged them to compare with each other. First, we arranged tsunami heights of five major tsunamis which occurred after the modern times (2011 Tohoku-oki, 1896 Meiji Sanriku, 1933 Showa Sanriku, 1968 Tokachi-oki, 1960 Chile). Then we compared these major tsunamis with historical tsunamis that recorded damages along the Iwate coast. According to comparison between major tsunamis, 2011 Tohoku-oki is highest in most part of the coast of Iwate Prefecture. However, 1896 Meiji Sanriku is almost the same as 2011 Tohoku-oki along the northern coast, and higher than 2011 Tohoku-oki at several sites.

1896 Meiji Sanriku and 1933 Showa Sanriku recorded large tsunami at the Yoshihama Bay, the Ryori Bay and the Hirota Point. These records might mean exaggeration or suggest conditions that amplified tsunami.

Although tsunami heights that documented in the "Yamana Reports" is almost matching with other records, unusual heights are shown at several sites. These records might include exaggeration based on folklore.

1968 Tokachi-oki and 1960 Chile tsunami are almost lower than 5m throughout the coast of Iwate Prefecture. These tsunamis show a trend which heights are a little higher at inside than the mouth of the bay.

1611 Keicho Oushu (Sanriku) tsunami recorded large tsunami at the Tanohata, Iwaizumi, Taro Coast and the Funakoshi, Yoshihama, Okirai Bay. Because large tsunami was recorded along southern coast of Iwate, the trend of tsunami heights distribution is similar to 2011 Tohoku-oki.

Although there are no records of definite damage by 869 Jogan tsunami in ancient documents along the Iwate coast, the distribution of tsunami deposits suggest that this tsunami might be large as 2011 Tohoku-oki.

Tsunami heights of 1856 Ansei, 1763 Hohreki, 1677 Enpoh tsunami which source located in northern part of Japan Trench show similar trend to 1968 Tokachi-oki. The effect of these tsunamis seems small along the Iwate coast. However, Tsunami height might be over 10m high on the coastal condition because 1677 Enpoh tsunami recorded 13m at Settai site. 1793 Kansei tsunami is also small relatively along the Iwate coast except for 9m at Ryoishi site.

Keywords: tsunami height, "Japan Tsunami Trace database", historical tsunami, Jogan tsunami, Jogan tsunami, Keicho Oushu (Sanriku) tsunami, Iwate Prefecture

The effective PML absorbing boundary condition for linear long-wave and linear dispersive wave tsunami simulations

*Takuto Maeda¹, Hiroaki Tsushima², Takashi Furumura¹

1.Earthquake Research Institute, the University of Tokyo, 2.Meteorological Research Institute, Japan Meteorological Agency

Tsunami simulations in regional scale usually performed in the bounded domain with appropriate absorbing boundary condition surrounding the computational area, for avoiding fictitious reflections from the model boundary contaminates the simulated tsunami wavefield. For such purpose, the Sommerfeld or the sponge boundary conditions are widely used. In the present study, we report that the new Perfectly Matched Layer condition, originally proposed in electromagnetics and being used widely in earthquake seismology, applied to the tsunami numerical simulation problem gives significant improvement on the quality of the boundary condition.

The PML is a sort of the sponge boundary condition, which damps outgoing tsunami waves by absorbing layer placed surrounding the numerical model with a finite thickness. In this PML region, physical variables were decomposed into directions according to the directions of their derivatives. Then, only a wave propagating perpendicular to the model boundary is absorbed so as to avoid artificial reflection from the boundary. A wave propagating parallel to the boundary is unchanged. This decomposition is a key to provide high-quality on absorbing outgoing waves without fictitious reflection. The linear-long wave tsunami perfectly suite the PML condition. In the case of the linear dispersive tsunami, however, the decomposition is not straightforward because the momentum equation contains a term of higher-order derivatives along the mixed directions. Therefore, we introduced a weighting factor in the PML absorber region, so that the effect of tsunami dispersion is gradually decreased as the tsunami penetrates towards the absorber region. Under this assumption, tsunami equation approaches to the linear long-wave equation, which enable us to utilize the PML equation.

To examine the efficiency of the proposed PML absorbing boundary conditions for numerical simulation of a tsunami, we performed a finite difference simulation tests under smooth and realistic bathymetry models using the PML condition. For comparison, we also simulated the tsunami with the use of the Sommerfeld radiation condition and a traditional sponge condition. In addition, we performed a simulation with a larger, boundary-free model for the reference. In both cases, the tsunami simulation with PML boundary condition shows significantly improved results having little fictitious reflection from boundaries. The Sommerfeld radiation condition in particular shows degraded performance for strongly dispersive waves. This is due to the mismatch between the dispersed various tsunami velocity and long-wave tsunami velocity assumed in the condition. The sponge boundary shows moderate performance, however it tends to have strong fictitious reflection for near-parallel angle incidence to the boundary. The PML boundary was always superior, even for the approximate implementation used in the linear dispersive waves.

In the regional tsunami modeling, the absorbing boundary is usually set at offshore where the water is deep. Therefore, the fictitious reflection at the boundary quickly come back to the model area with increasing amplitude as the water gets shallower, and it easily contaminate the model area. Because the computational loads for linear long-wave tsunami simulation is not so heavy for recent computers, one might extend the model area to avoid such reflection. However, the same procedure for the linear dispersive waves is not realistic, because its computational cost is 50-100 times as high as that for the linear long wave tsunami. The proposed PML boundary condition significantly improve the quality of tsunami numerical modeling without increasing computational cost.

Keywords: Tsunami, Numerical simulation, Finite difference method, Absorbing boundary condition, PML

Simulation of the 2011 Tohoku earthquake including rupture process of seafloor motion and wave dispersion

*Yoshinori Shigihara¹, Yasuko Hiwatashi²

1.National Defense Academy, 2.Tokyo University of Marine Science and Technology

The 2011 Tohoku earthquake tsunami gave us a lot of physical data to study the generation process of mega-tsunami. After this event, tsunami scientists tried to make an initial tsunami source model by using tsunami waveform inversion analysis, so that some of models are used for the tsunami damage estimation in practice. Although a number of seismic source models also have been derived by seismologists by using geodetic data, teleseismic data and strong motion data, few studies used their models for the tsunami simulation. It is generally believed that fault models, which are determined by the tsunami inversion analysis and by the seismic inversion analysis, do not correspond with each other, however a series of phenomena such as earthquakes and tsunamis should be expressed as a single model. In this study, we conducted a numerical simulation of the 2011 Tohoku tsunami using the seismic source model, and discuss an importance of considering rupture processes of seafloor motion and wave dispersion effects of tsunami propagation.

In order to describe tsunami generation from detailed seafloor deformation, we adopted the seismic source model by Yagi and Fukahata (2011), which is estimated the rupture process from teleseismic P-wave data using the newly inverse method that takes into account the uncertainty of the Green's function. This model provides rupture velocity and rise time to prescribe kinematic seafloor deformation with the planar fault model of Mansinha and Smylie (1971). Tsunami waves are computed using the dispersion potential model (Shigihara and Fujima, 2014), which is based on the staggered leap-frog implicit scheme; dispersive terms in the equation of motion is solved separately. The grid nesting method that we newly developed for the dispersion potential model are used for the bathymetry dataset with three levels of grid resolution (1350m, 450m and 150 m). The computed results were compared to the time history of the sea surface elevation observed at GPS buoys where are located along off the Sanriku coast. Considering the rupture velocity and the rise time makes the tsunami generation process slowly, and contributes the reproducibility of overall wave profiles. In addition, the wave dispersion effects on decrease of the leading wave height. The computed results agree well with observation, we found that both of the physical processes, that is the rupture process of the seafloor and the dispersion effect, must be considered if we want to simulate tsunami propagation using the seismic source model precisely.

Keywords: 2011 Tohoku Tsunami, tsunami simulation

Database construction of Tsunami inundation zone for large subduction-zone earthquakes: A case of Ishinomaki City

*Seiji Tsuno¹, Kyosuke Okamoto¹, Norihiko Hashimoto², Satoru Fujihara², Mariko Korenaga²

1.Railway Technical Research Institute, 2.ITOCHU Techno-Solutions Corporation

Real-time prediction of Tsunami in a coastal zone (Tsushima et al., 2009) is quite effective for an early warning, in terms of lead time to be evacuated from the coastal zone and to understand the tsunami water level; however, this information is not accessible to the citizens and various companies. To issue the better Tsunami early warning, Tsunami inundation zones should be visualized by database of Tsunami inundation zones for large subduction-zone earthquakes (Honma and Katada, 2009), in which Tsunami inundation zones are related to tsunami water levels in the coastal zones. In this report, for an example of Ishinomaki City, Miyagi Pref., we constructed database of Tsunami inundation zone for large subduction-zone earthquakes along Japan Trench. We simulated Tsunami inundation in Ishinomaki City for 27 models of scenario Tsunami sources (the Headquarters for Earthquake Research Promotion, 2011), which set on large subduction-zone earthquakes (M8-9) in Tohoku-Oki. In the simulation, we applied the non-linear long-wave theory, with a grid size of 1215m / time interval 0.9s in the sea and a grid size of 15m / time interval 0.1s in the land. We applied crustal deformations after Okada (1992) to initial water levels, in the boundary conditions of the perfect transmission in the sea and runup in the land (Kotani, 1998). In the future, we will investigate real-time prediction of Tsunami inundation zone by the matching method for the database of Tsunami inundation zones and tsunami water levels in the coastal zones.

Keywords: Tsunami inundation zone, Database, Ishinomaki City

A prototype of database-driven system for tsunami inundation prediction using the JMA's disaster information XML

*Toshitaka Baba¹, Makoto Bando²

1.Institute of Technology and Science, The University of Tokushima, 2.Tokushima Prefecture

The Nankai earthquakes are anticipated to occur accompanied by large tsunamis. Emergency disaster operations should be started rapidly and properly to save lives after the great tsunami disasters happen. In order to enhance the emergency disaster operation, we need to provide a possible tsunami inundation area as soon as possible. Although a site survey will be conducted after a half day or a day by using a helicopter for example, numerical tsunami predictions using the real-time seismic and tsunami observation are solely available until the first 12 hours to draw a big picture of the disaster. This study developed a prototype predicting tsunami inundation to the coastal area in Tokushima prefecture. The basic algorithm of prototype is similar with that of the national tsunami early warning system in Japan that selects an appropriate earthquake scenario from pre-computed tsunami database based on the epicentral location and magnitude. A difference between the JMA's system and this study can be seen in prediction target. They predict tsunami height at the coast line, but our system will predict tsunami inundation on land. We applied an open source platform, JoruriDms, to carry out the prototype. JoruriDms is a disaster management system equipped with GIS and various functions to support operations of the local government during disaster, which has been already used in the Tokushima prefecture. We defined about 220 earthquake scenarios possibly occurred in the Nankai subduction zone with a range of magnitude from 6.5 to 9.0. We here assumed heterogeneous slips on the fault planes. We repeatedly calculated tsunamis by changing the earthquake scenarios to evaluate tsunami inundation on land with spatial resolution of 5 m interval. All data were stored in a tsunami database. A logic tree was constructed to select only one scenario from the tsunami database based on the epicentral location and magnitude provided by the JMA's disaster information XML. However, this algorithm doesn't take into account earthquake rupture extent. It is also not good at tsunami earthquake which generates a large tsunami with weak seismic shaking. We accordingly added a function to upgrade (re-select) scenario based on tsunami height observations off shore and at the coast, which are provided by follow-up information of the JMA's XML. We will also discuss further plans in the presentation to improve the prediction accuracy by increasing number of the earthquake scenarios and adopting real-time data provided by the ocean bottom pressure array (DONET) in the Nankai trough.

Keywords: Tsunami, Early prediction

Feature extraction from result of tsunami simulation by applying image analysis

*Takeyasu Yamamoto¹

1.Meteorological Research Institute

In this report, some interpretation methods of tsunami height distribution obtained by tsunami propagation simulation are tested. A wave crest, which is a typical feature of tsunami height distribution, is equivalent to a ridge in landform, so the methods used in landform analysis or image analysis are expected to be utilized to extract wave crest. In the case that Laplacian operator is applied, extracted region is broad in rise while disconnect in col, which is depend on selection of threshold. Application of median filter extracts wave crest successfully, including secondary wave crest formed by refraction effect. However, grids on which tsunami heights aren't local maxima are also extracted, so it needs to examine other type of filters.

Validation for tsunami source model of large earthquakes occurred in the Sea of Japan

*Satoko Murotani¹, Kenji Satake², Tomoya Harada²

1.National Museum of Nature and Science, 2.Earthquake Research Institute, the University of Tokyo

For the 1964 off Oga Peninsula (Mjma 6.9), 1971 West off Sakhalin (Mjma 6.9), 1983 West off Aomori (Mjma 7.1) earthquakes occurred in the Sea of Japan, tsunami waveforms are computed and compared with the recorded ones on tide gauges for the heterogeneous slip models obtained by the teleseismic waveform inversion and tsunami source models compiled by MLIT (Ministry of Land, Infrastructure, Transport and Tourism), CAO (Cabinet Office), and MEXT (Ministry of Education, Culture, Sports, Science and Technology) (hereinafter referred to as "MLIT model") (Murotani et al., 2015, JpGU; 2015, SSJ). As the results, the calculated tsunami waveforms were almost the same whether the dispersion term is included or not in the simulation, and whether the slip on faults is heterogeneous or uniform. In this study, we quantitatively compare the observed tsunami waveforms with the calculated tsunami waveforms to examine the validity of those fault models. It is difficult to compare the entire waveforms of M7 class tsunami, because the later part of waveforms may have an influence due to a bay or a shelf where tide gauge stations locate. In this study, we used factors K and k by Aida (1978, JPE). K is the geometrical mean value of K_i , where K_i is the ratio of the observed and the calculated amplitudes for the first wave and the second one of i th stations, and $\log k$ is the logarithmic standard deviation of K_i .

For the 1964 earthquake, we estimated K and k for six fault models which are the teleseismic waveform inversion model and some modified MLIT models, etc. k was the smallest (1.65) for a rectangular fault with uniform slip of 0.4 m, that is larger than the average slip 0.2 m of the heterogeneous slip distribution (fault size: 50 km x 40 km, M_0 : 1.5×10^{19} Nm, maximum slip: 1.4 m) obtained by the teleseismic waveform inversion. This uniform slip 0.4 m best reproduced the amplitudes of the observations ($K = 1.11$). For the 1971 earthquake, we estimated K and k for five fault models which are the teleseismic waveform inversion model and modified uniform slip models. k was relatively small (2.42) for both the first and the second waves from the heterogeneous slip distribution (fault size: 50 km x 30 km, M_0 : 1.3×10^{19} Nm, maximum slip: 1.2 m, average slip: 0.2 m) obtained by the teleseismic waveform inversion. However, the amplitudes of the calculated waveforms was so small ($K = 2.41$). The amplitudes of the observations were reproduced ($K = 1.13$) when we assumed the rectangular fault with uniform slip 0.5m, although k was a little larger (2.80). If only the first wave is used, k was the smallest (2.01) from two rectangular faults (fault size: 30 km x 20 km and 30 km x 20 km) with uniform slip 0.2 m and 1.5 m, respectively. The strike 21° of this model was changed from the strike 329° obtained by the teleseismic waveform inversion. However, k values of this earthquake are still large, hence further examination is necessary. For the 1983 earthquake, we estimated K and k for six fault models which are the teleseismic waveform inversion model and some modified MLIT models, etc. k was the smallest (1.64) from the heterogeneous slip distribution (fault size: 50 km x 30 km, M_0 : 3.1×10^{19} Nm, maximum slip: 2.2 m, average slip: 0.5 m) obtained by the teleseismic waveform inversion. This model best reproduced the amplitudes of the observations ($K = 1.33$) as well.

Keywords: eastern margin of the Sea of Japan, tsunami waveform analysis, fault parameters

Tsunami simulations toward probabilistic tsunami hazard assessment in the Nankai Trough

*JUMPEI TAKAYAMA¹, Tadashi Kitou², Norihiko Hashimoto³, Ryu Saito¹, Yasuhiro Murata¹, Takuya Inoue¹, Yoichi Murashima¹, Hisanori Matsuyama², Shinichi Akiyama³, Hiromitsu Nakamura⁴, Kenji Hirata⁴, Hiroyuki Fujiwara⁴

1.KOKUSAI KOGYO CO., LTD., 2.OYO Corporation, 3.CTC, 4.NIED

NIED began a research project regarding probabilistic tsunami hazard assessment (PTHA) for Japan since 2012 (Fujiwara et al., 2013, JpGU). Hirata et al. (2014, JpGU) reported the concept of this study that a nation-wide PTHA is to be obtained by aggregating evaluations performed for each region-wide PTHA such as shorelines along the Nankai Trough, the Japan Trench, etc. A region-wide PTHA is to analyze coastal hazard caused by tsunami wave heights estimated with a numerical simulation. Here, we show preliminary datasets of coastal tsunami wave heights in the shorelines between Kagoshima and Ibaraki prefectures computed by thousands of fault models on assumption of possible scenarios for Nankai Trough earthquakes.

We focus on Nankai Trough earthquakes which there are a concern that tsunami may arrive at coastal regions in future. Our research target includes not only the subduction earthquakes that are mainly considered by the possible tsunami-genic earthquake derived from a seismic slip on a plate boundary in subduction zone but also unspecified fault sources such as small and medium scale earthquakes. Toyama et al. (2015, JpGU) and Hirata et al. (2015, SSJ Fall Meeting) introduced how to build up a set of characterized earthquake fault models (CEFMs) on hypothesized earthquakes along the Nankai Trough, referring to the "Long-term Evaluation of earthquakes in the Nankai Trough region (2nd edition)" by the Headquarters for Earthquake Research Promotion (HERP, 2013), where we constructed a set of the 1442 simplified fault models in the 15 types of source regions described in the long-term evaluation, i.e. 1) the 24 basic fault models, in which we put a large slip area (LSA) on the basis of the configuration of the previous studies for the historical large earthquakes along the Nankai Trough, 2) the 1411 extended fault models, in which we put LSAs for variety of fault models, and 3) the 7 recurrence fault models, in which we put the source area corresponding to the historical tsunami-genic earthquakes evaluated by HERP. Additionally, a set of the other 2455 extended fault models in the other 70 types of source regions are newly constructed in this study. Then, the total number of the CEFMs reaches a little less than 4000.

With the around 4000 fault models, initial wave heights are calculated from surface deformation via Okada's equation (Okada, 1992). A tsunami run-up simulation estimates tsunami wave heights along Pacific coast from Kagoshima to Ibaraki prefectures, solved by the non-linear shallow-water equation using a leap-frog scheme. These simulations are configured by a nested grid system consisting of four sub-regions from outer 1350 m to inner 50 m in a horizontal, landward inundation keeping, and transparent at the seaward edges.

The preliminary datasets of coastal tsunami wave heights contribute to implementing uncertainty into coastal probabilistic tsunami hazard (Abe et al., 2015, JpGU) and to constructing a database. This study was done as a part of the research project on probabilistic tsunami hazard assessment (PTHA) for Japan area by NIED.

Keywords: Probabilistic tsunami hazard assessment (PTHA), Tsunami simulation, the Nankai Trough, Database

Probabilistic Tsunami Hazard Assessment along the Nankai Trough considering the diversity of earthquake fault models

*Yuta Abe¹, Mariko Korenaga¹, Shinichi Akiyama¹, Hisanori Matsuyama², Yasuhiro Murata³, Kenji Hirata⁴, Hiroyuki Fujiwara⁴

1.ITOCHU Techno-Solutions Corporation, 2.OYO-corporation, 3.KOKUSAI KOGYO CO., LTD, 4.National Research Institute for Earth Science and Disaster Prevention

We have conducted a probabilistic tsunami hazard assessment along the Nankai trough on the basis of The Earthquake Research Committee(ERC)/HERP, Government of Japan (2013). From the experience of 2011 Tohoku earthquake, ERC(2013) revised their long-term evaluation of the forthcoming large earthquake along the Nankai Trough from specifying earthquake sources and magnitudes to considering the diversity of earthquake source. ERC(2013) exemplified 15 hypothetical source areas which were thought as source areas of historical earthquakes. We constructed characterized earthquake fault models on each of the hypothetical source areas (Toyama et al., 2015) and calculated tsunami hazard curves at every evaluation points on coasts (Hirata et al., 2015; Korenaga et al., 2015).

In this study, we extend the hypothetical source areas from those exemplified by ERC(2013) to every possible source areas including those where earthquake occurrence yet to be identified and update a probabilistic tsunami hazard assessment along the Nankai trough. The total number of the hypothetical source areas is 85 and the number of the characterized earthquake fault models is 3928. We set probabilistic weights for each characterized earthquake fault models as follows:

- i) For the 15 hypothetical source areas exemplified by ERC(2013), weights are calculated by following a probability re-distribution concept (ERC,2014).
- ii) For the other hypothetical source areas larger than 3 segments, we classify them 15 groups which are recognized as parts of hypothetical source areas exemplified by ERC(2013), and divide the weights.
- iii) For the hypothetical source areas smaller than 2 segments, we assume that their occurrence obeys a Gutenberg-Richter model calculated by the past seismic activity around the Nankai trough.

Keywords: tsunami hazard assessment, probability, Nankai trough, long-term evaluation, tsunami simulation